ΥΠΟΥΡΓΕΙΟ ΠΕΡΙΒΑΛΛΟΝΤΟΣ, ΧΩΡΟΤΑΞΙΑΣ & ΔΗΜΟΣΙΩΝ ΕΡΓΩΝ
ΓΕΝΙΚΗ ΓΡΑΜΜΑΤΕΙΑ ΔΗΜΟΣΙΩΝ ΕΡΓΩΝ
Δ/ΝΣΗ ΕΡΓΩΝ ΥΔΡΕΥΣΗΣ & ΑΠΟΧΕΤΕΥΣΗΣ

ΕΘΝΙΚΟ ΜΕΤΣΟΒΙΟ ΠΟΛΥΤΕΧΝΕΙΟ

ΤΟΜΕΑΣ ΥΔΑΤΙΚΩΝ ΠΟΡΩΝ ΥΔΡΑΥΛΙΚΩΝ & ΘΑΛΑΣΣΙΩΝ ΕΡΓΩΝ

MINISTRY OF ENVIRONMENT, REGIONAL PLANNING & PUBLIC WORKS
GENERAL SECRETARIAT OF PUBLIC WORKS
SECRETARIAT OF WATER SUPPLY & SEWAGE

NATIONAL TECHNICAL UNIVERSITY OF ATHENS
DIVISION OF WATER RESOURCES HYDRAULIC & MARITIME ENGINEERING

ΕΡΕΥΝΗΤΙΚΟ ΕΡΓΟ
ΕΚΤΙΜΗΣΗ ΚΑΙ ΔΙΑΧΕΙΡΙΣΗ ΤΩΝ ΥΔΑΤΙΚΩΝ ΠΟΡΩΝ ΤΗΣ ΣΤΕΡΕΑΣ ΕΛΛΑΔΑΣ

ΦΑΣΗ Γ

ΤΕΥΧΟΣ 39

ΑΝΑΠΤΥΞΗ ΜΟΝΤΕΛΟΥ ΠΡΟΣΟΜΟΙΩΣΗΣ ΚΑΙ ΒΕΛΤΙΣΤΟΠΟΙΗΣΗΣ ΥΔΡΟΣΥΣΤΗΜΑΤΟΣ ΔΥΤΙΚΗΣ ΣΤΕΡΕΑΣ ΕΛΛΑΔΑΣ

RESEARCH PROJECT
EVALUATION AND MANAGEMENT OF THE WATER RESOURCES OF STEREA HELLAS

PHASE C

VOLUME 39

MODEL DEVELOPMENT FOR SIMULATION AND OPTIMISATION OF THE WESTERN STEREA HELLAS HYDROSYSTEM

ΣΥΝΤΑΞΗ: Α. ΓΕΩΡΓΑΚΑΚΟΣ, Η. ΥΑΟ, C.DEMARCHI, M. MULLUSKY

ΕΠΙΣΤΗΜΟΝΙΚΟΣ ΥΠΕΥΘΥΝΟΣ: Δ. ΚΟΥΤΣΟΓΙΑΝΝΗΣ
ΚΥΡΙΟΣ ΕΡΕΥΝΗΤΗΣ: Ι. ΝΑΛΜΠΑΝΤΗΣ

BY: A. GEORGAKAKOS, H. YAO, C.DEMARCHI, M. MULLUSKY

SCIENTIFIC DIRECTOR: D. KOUTSOYIANNIS
PRINCIPAL INVESTIGATOR: I. NALBANTIS

ΑΘΗΝΑ - ΙΑΝΟΥΑΡΙΟΣ 1999

ATHENS - JANUARY 1999

School of Civil and Environmental Engineering

A Decision Support System for the Western Sterea Hellas Water Resources System

Developed by

Aris Georgakakos
Huaming Yao
Carlo DeMarchi
Mary Mullusky

Georgia Water Resources Institute
Atlanta, Georgia 30332, USA

in collaboration with

The National Technical University of Athens

Developed for

The Greek Ministry of Environment, Regional Planning, & Public Works (ΥΠΕΧΩΔΕ)

December 1998

CONTENTS

Chapter

CHAPTER 1

INTRODUCTION

Thessalia valley is in central Greece and is a key agricultural region for the national economy. However, in recent years, the impacts of population growth and agricultural expansion have resulted in frequent droughts, diminishing water supplies, and ecosystem degradation. To reverse this trend and to maintain the sustainability of the land resources, a water diversion has been proposed from the nearby Acheloos River Basin. The diversion is planned to take place from Sykia, a new reservoir currently being constructed at the upper reaches of the Acheloos River. Figure 1.1 schematically depicts the existing and planned hydraulic works that would enable this inter-basin water transfer. The features of these projects are described in the following section.

Previous studies (*Georgakakos, et al., 1995*) have shown that a diversion of 600 million cubic meters per year would reduce energy generation at the existing hydropower facilities of the Acheloos River (Kremasta, Kastraki, and Stratos) by about 15% per year, without significantly affecting the other water uses in the Acheloos Basin. However, this is a partial assessment, and more detailed studies are needed to evaluate the overall impacts and benefits of the water resources system to be created after the diversion is in place.

With this background, the purpose of this study is to develop a mathematical model that incorporates all major elements of the new system configuration and use it to carry out the aforementioned integrated assessments. The model includes a control (i.e., optimization) and a control-simulation component. The purpose of the control model is to develop optimal reservoir operation policies, while that of the control-simulation model is to evaluate the performance of these policies over the historical (or a synthetically generated) inflow record.

The report includes five chapters and three appendices. In the following chapter, we give a short overview of the Western Sterea Hellas reservoir system and discuss the data used in the study. In Chapter 3, we introduce the control model formulation, discuss our modeling

assumptions, and briefly describe the basis of the optimization methodology implemented in this decision support system. In Chapter 4, we present and elaborate on the model results, and in Chapter 5 we summarize the most important conclusions and make suggestions for further investigations. The appendices contain auxiliary information such as reservoir characteristic curves, the pump-storage representation of the Pefkofito hydropower station, and tables with more detailed results of the model runs.

A reader interested in the implications of the study relative to the proposed diversion may wish to read Chapter 2 to become familiar with the system configuration and project features, and then proceed to Section 4.2 where we provide a critical discussion of the assessment investigations. The more technically-oriented reader should also review Chapter 3 which describes the mathematical model developed for and used in these assessments. Lastly, this model is a part of a user-friendly decision support software which may be used for a series of similar investigations and sensitivity studies. This software is described separately in a user manual.

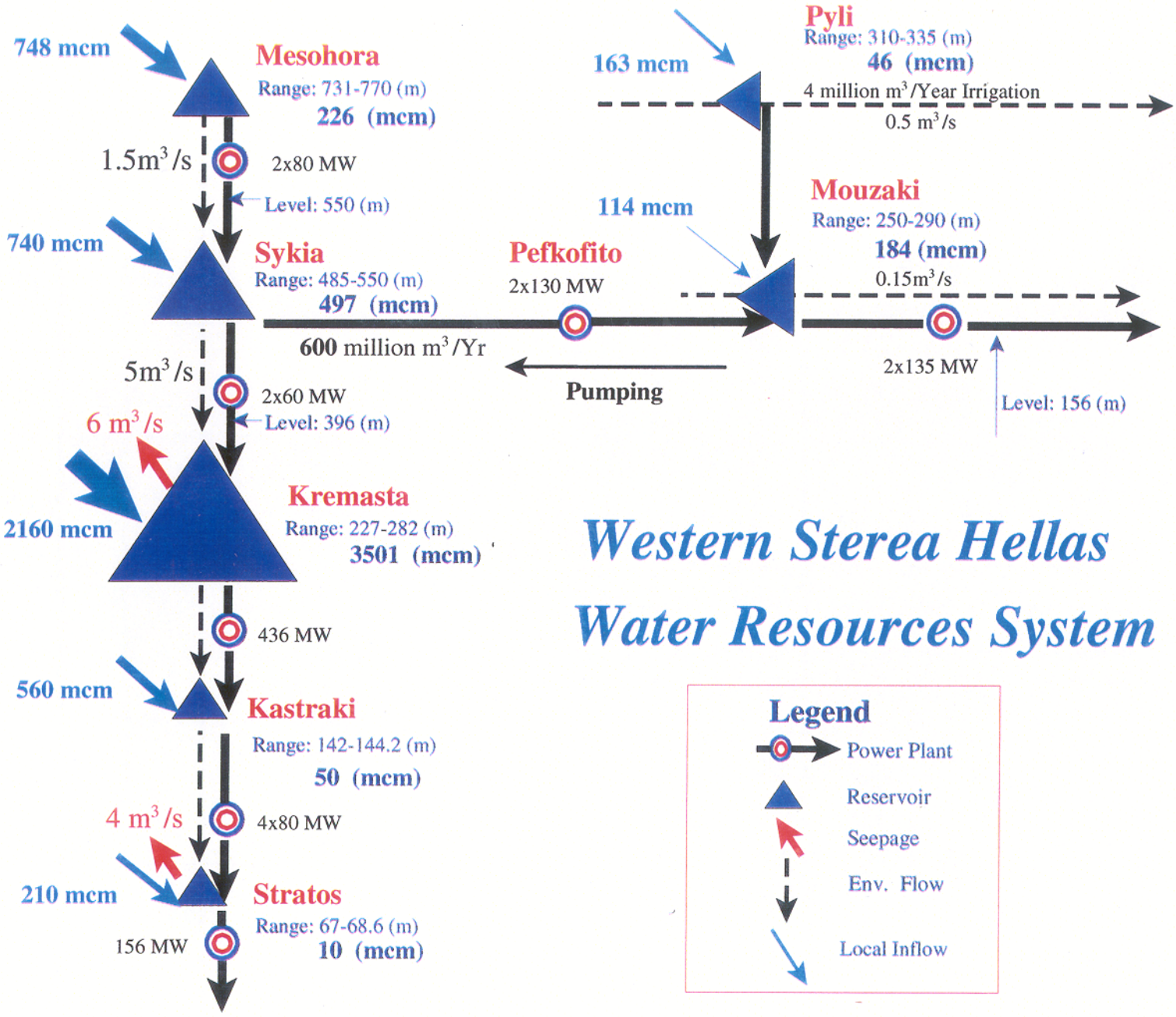

Figure 1.1: The Western Sterea Hellas Reservoir System

CHAPTER 2

THE WESTERN STEREA HELLAS RESERVOIR SYSTEM

The Acheloos River Basin (Figure 1.1) currently includes three reservoirs (Kremasta, Kastraki, and Stratos), while two other projects (Mesohora and Sykia) are presently under construction. Of the existing reservoirs, the largest is Kremasta with a total storage of $4{,}500 \times 10^6$ cubic meters, whereas the others are smaller projects with a combined storage of less than $1{,}500 \times 10^6$ cubic meters. The proposed water diversion to Thessalia would take place from the Upper Acheloos (Sykia). The water works associated with the diversion also include two new reservoir at Mouzaki and, possibly, at Pyli. The conservation storage of these reservoirs is used to support water supply, hydropower generation, and environmental protection and is reported in Table 2.1.

Table 2.1: Conservation Storage Ranges

Reservoir	Minimum		Maximum	
	Storage (10^6 m^3)	Elevation (m)	Storage (10^6 m^3)	Elevation (m)
Mesohora	132.8	731	358	770
Sykia	94	485	590.8	550
Kremasta	999	227	4500	282
Kastraki	750	142	800	144.2
Stratos	60	67	70.2	68.6
Pyli	21.7	310	125.4	355
Mouzaki	54.4	250	237.2	290

Average seepage losses amount to 6 m^3/sec at Kremasta and 4 m^3/sec at Stratos, while at other projects, they are either negligible or unavailable. Other reservoir data, including elevation

versus storage and area versus storage curves, are included in Appendix A. All projects except Pyli have hydroelectric generation units, the number and capacities of which are shown on Table 2.2.

Table 2.2: Hydroelectric Plant Characteristics

Reservoir	(**Number of Units**) x (**Installed Capacity** - MW)
Mesohora	2 x 80
Sykia	2 x 60
Kremasta	4 x 109 = 436
Kastraki	4 x 80 = 320
Stratos	2 x 75 + 2 x 3 = 156
Pyli	0
Mouzaki	2 x 135
Pefkofito	2 x 130

The water diversion from Sykia to Mouzaki passes through the power facility at Pefkofito. The turbines at Pefkofito can also operate in a pumping mode. Approximate relationships among power generation, reservoir elevation, and turbine discharge are provided in Appendix A for all power facilities. For lack of more detailed data, these relationships are used herein to model power generation at the monthly time scale.

Figures 2.1, 2.2, and 2.3 respectively summarize the monthly statistics of reservoir inflows (local drainage basins) for all reservoirs. The previous statistics are based on a 32-year record, extending from 1961 to 1993. Tables 2.3 and 2.4 report the monthly statistics of the evaporation and rainfall rates for all reservoirs based on the same historical period.

Table 2.3: Monthly Evaporation Rate (mm)

Month	Mesohora	Sykia	Kremasta	Kastraki	Stratos	Pyli	Mouzaki

Jan	35.2	37.5	33.370	33.370	33.370	40.8	41
Feb	34.8	40.8	52.860	52.860	52.860	40.3	44.6
Mar	53.3	56.5	79.380	79.380	79.380	61.5	61.6
Apr	68.3	74.7	119.99	119.99	119.99	78.5	81.3
May	115.3	122.3	162.94	162.94	162.94	131.9	132.7
Jun	169.1	185.5	206.24	206.24	206.24	192.6	200.7
Jul	222.7	236.5	237.79	237.79	237.79	252.9	255.4
Aug	176.9	187.8	212.18	212.18	212.18	201	202.9
Sep	123.3	135.3	147.19	147.19	147.19	140.4	146.4
Oct	57.8	61.2	76.010	76.010	76.010	66.2	66.4
Nov	32.2	35.2	38.500	38.500	38.500	37.1	38.3
Dec	32.4	34.4	25.570	25.570	25.570	37.4	37.6

Table 2.4: Monthly Rainfall Rate (mm)

Month	Mosohora	Sykia	Kremasta	Kastraki	Stratos	Pyli	Mouzaki
Jan	223.04	266.65	149.18	134.45	134.45	207.49	194.09
Feb	212.66	251.06	144.55	136.78	136.78	200.61	175.27
Mar	159.56	184.66	115.17	104.32	104.32	161.85	143.27
Apr	133.80	158.36	95.880	78.790	78.790	144.87	125.73
May	101.20	109.24	72.310	51.170	51.170	104.88	86.61
Jun	48.060	53.460	37.620	33.730	33.730	43.520	40.54
Jul	36.750	39.060	23.300	18.600	18.600	28.040	25.53
Aug	34.200	45.060	20.100	22.860	22.860	33.900	29.77
Sep	64.790	75.440	50.030	42.790	42.790	60.350	57.36
Oct	165.00	174.91	108.29	103.88	103.88	181.36	154.15
Nov	255.52	293.29	216.31	206.34	206.34	225.85	197.54

Dec	295.99	340.50	210.69	187.13	187.13	287.74	245.11

Except for energy generation and flood protection, this reservoir system is expected to provide water for irrigation and maintain sufficient in-stream flows to preserve environmental quality. At Stratos, irrigation release amount to 35 m^3/sec during May through September, while 21 m^3/sec are mandated throughout the year for environmental protection. Thus, the minimum release from Stratos is 56 m^3/sec for May through September and 21 m^3/sec for the rest of the year. The annual irrigation requirement for Pyli is 4 million cubic meters distributed from April through September. The environmental release requirements are 0.5 and 0.15 m^3/s, respectively, for Pyli and Mouzaki. Table 2.5 reports the combined release constraints for all reservoirs.

Table 2.5: Monthly Release Constraints (m^3/s)

	Mesohora	Sykia	Kremasta	Kastraki	Stratos	Pyli	Mouzaki
Jan	1.5	5	0	0	21	0.5	0.15
Feb	1.5	5	0	0	21	0.5	0.15
Mar	1.5	5	0	0	21	0.5	0.15
Apr	1.5	5	0	0	21	0.58	0.15
May	1.5	5	0	0	56	0.67	0.15
Jun	1.5	5	0	0	56	0.86	0.15
Jul	1.5	5	0	0	56	0.97	0.15
Aug	1.5	5	0	0	56	0.91	0.15
Sep	1.5	5	0	0	56	0.55	0.15
Oct	1.5	5	0	0	21	0.5	0.15
Nov	1.5	5	0	0	21	0.5	0.15
Dec	1.5	5	0	0	21	0.5	0.15

The proposed water transfer from the Acheloos Basin to the neighboring region of

Thessalia is planned to take place from Sykia to Mouzaki. The amount of the diversion is estimated at 600 million cubic meters annually, and its main purpose is irrigation. The expected irrigation demand of the Thessalia region has the distribution shown in Table 2.6 (percentage form).

Table 2.6: Seasonal Distribution of Irrigation Demand

Month	Jan-Mar	April	May	June	July	Aug.	Sep.	Oct-Dec
%	0	5	11	23.6	30.2	26.4	3.8	0

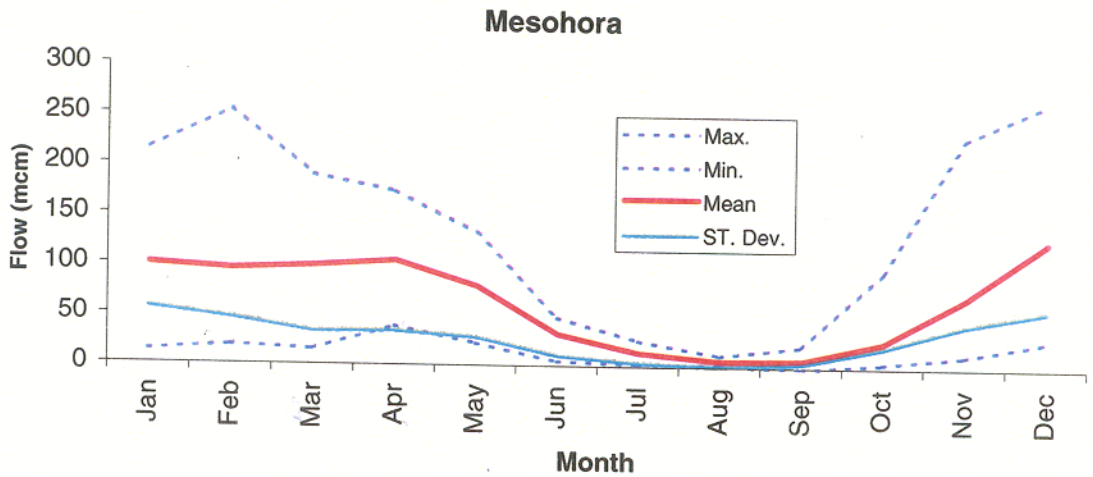

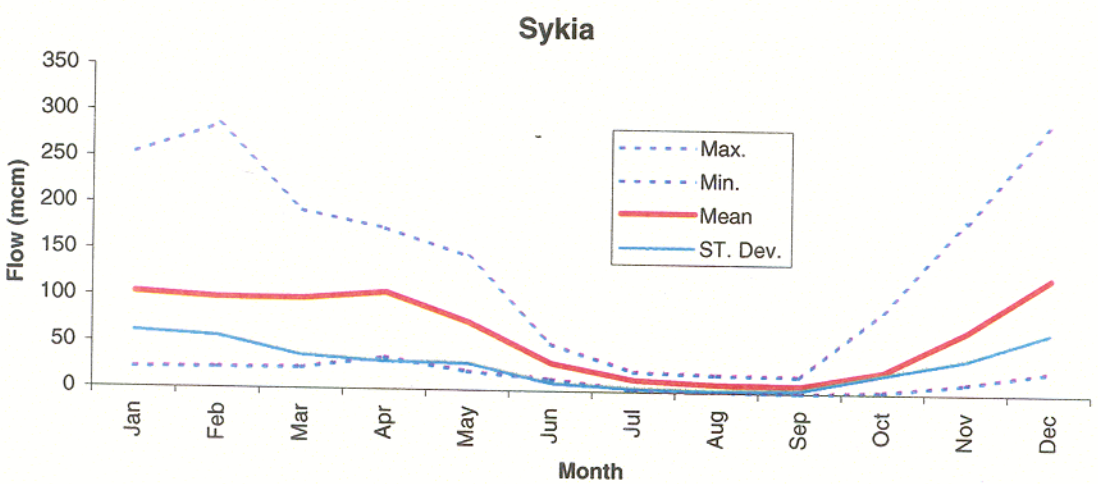

Figure 2.1: Inflow Statistics; Mesohora and Sykia

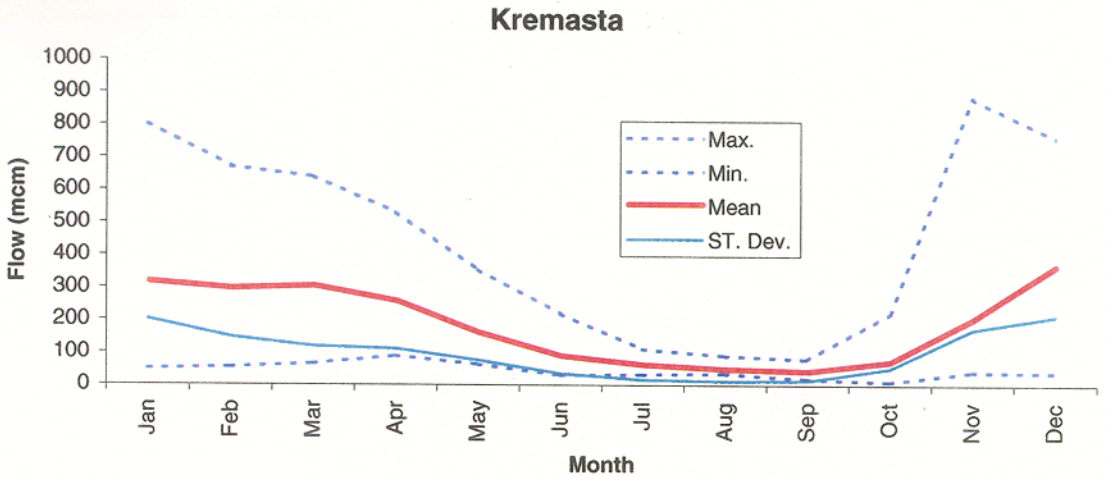

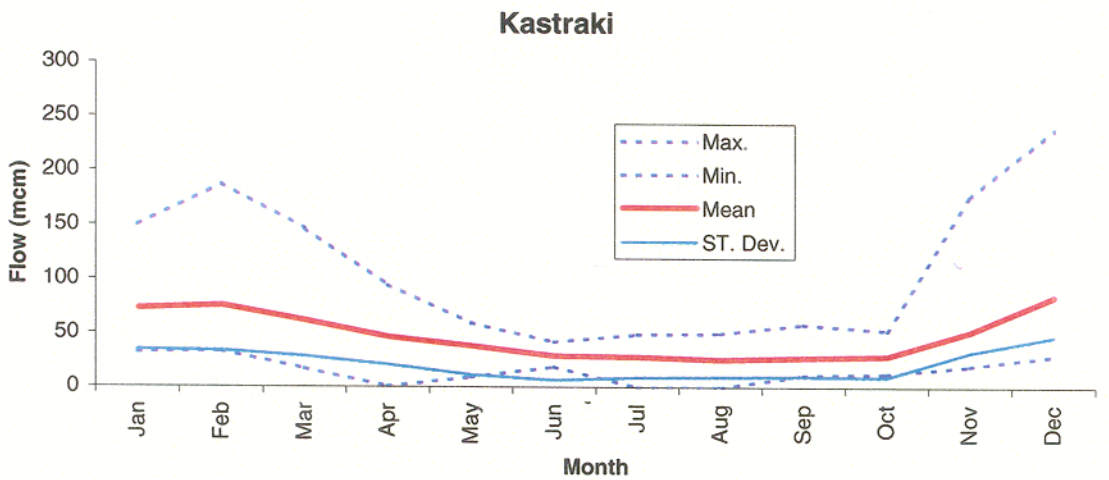

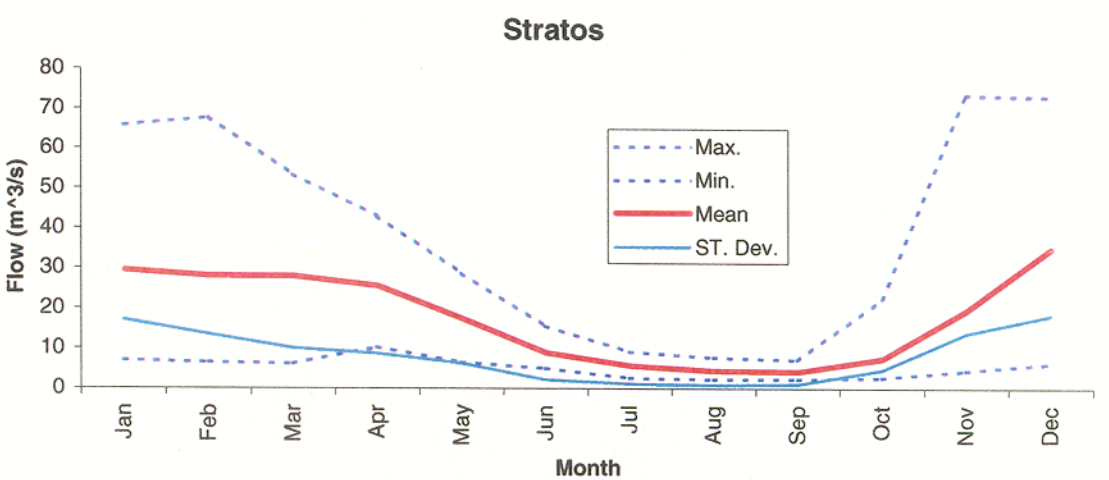

Figure 2.2: Inflow Statistics; Kremasta, Kastraki, and Stratos

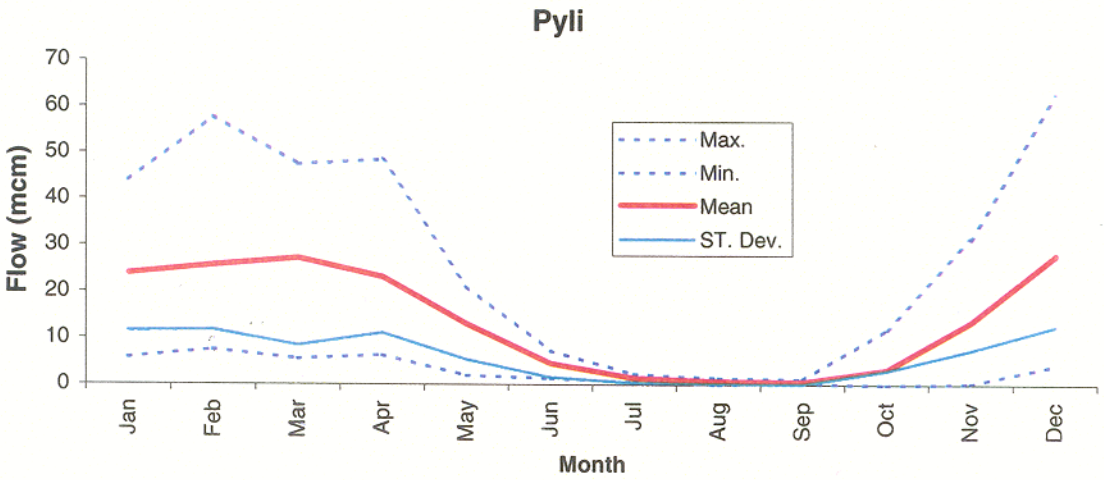

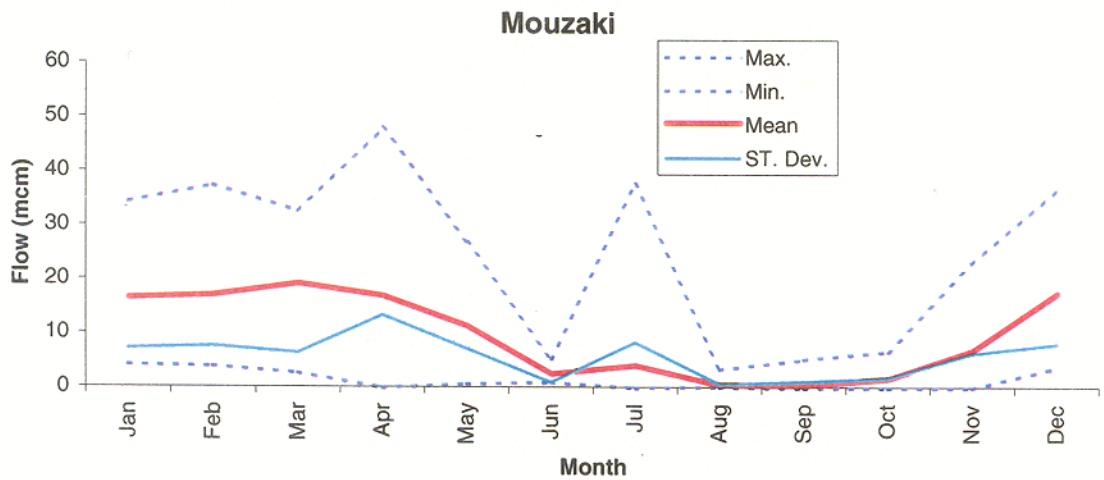

Figure 2.3: Inflow Statistics; Pyli and Mouzaki

CHAPTER 3

CONTROL MODEL

3.1 Formulation

3.1.1 System Dynamics

The Western Sterea Hellas reservoir system is modeled by the following water balance relationships:

$$
\begin{aligned}
S_1(k+1) &= S_1(k) - e_1(k)A_1[S_1(k)] - u_1(k) + w_1(k) - L_1(k) - EF_1(k) - D_1(k),\\
S_2(k+1) &= S_2(k) - e_2(k)A_2[S_2(k)] - u_2(k) + u_1(k) - u_8(k) + w_2(k) - L_2(k) + EF_1(k) - EF_2(k) - D_2(k),\\
S_3(k+1) &= S_3(k) - e_3(k)A_3[S_3(k)] - u_3(k) + u_2(k) + w_3(k) - L_3(k) + EF_2(k) - EF_3(k) - D_3(k),\\
S_4(k+1) &= S_4(k) - e_4(k)A_4[S_4(k)] - u_4(k) + u_3(k) + w_4(k) - L_4(k) + EF_3(k) - EF_4(k) - D_4(k),\\
S_5(k+1) &= S_5(k) - e_5(k)A_5[S_5(k)] - u_5(k) + u_4(k) + w_5(k) - L_5(k) + EF_4(k) - EF_5(k) - D_5(k),\\
S_6(k+1) &= S_6(k) - e_6(k)A_6[S_6(k)] - u_6(k) + w_6(k) - L_6(k) - EF_6(k) - D_6(k),\\
S_7(k+1) &= S_7(k) - e_7(k)A_7[S_7(k)] - u_7(k) + u_6(k) + u_8(k) + w_7(k) - L_7(k) - EF_7(k) - D_7(k)\\
S_8(k+1) &= S_8(k) + u_8(k),\\
k &= 0,1,\ldots,N-1\ ,
\end{aligned}
\qquad \textbf{(3.1)}
$$

where the subscripts i = 1 to 7 respectively denote quantities pertaining to Mesohora, Sykia, Kremasta, Kastraki, Stratos, Pyli, and Mouzaki; k is the discretization time interval corresponding to one month; $S_i(k)$ is the storage of the ith reservoir at the beginning of the month; $e_i(k)$ is the evaporation rate; $A_i[S_i(k)]$ is the reservoir area versus storage curve; $u_i(k)$ is the release volume over the period k; $w_i(k)$ is the inflow volume; $L_i(k)$ is the seepage loss; $u_8(k)$ is the net monthly transfer from Sykia to Mouzaki, representing the water diversion from the Acheloos Basin to the Thessalia region; $S_8(k)$ is an additional state variable representing the cumulative diversion volume from period 0 to period k; $EF_i(k)$ is the environmental flow requirement; $D_i(k)$ is the water withdrawal from the i^{th} reservoir, if any; and N is the control horizon in months. The environmental flows from Mesohora, Sykia, Pyli, and Mouzaki do not

pass through the power facilities while those of Stratos do. The 4 million cubic meters annual irrigation requirement from Pyli is modeled as a direct withdrawal from reservoir storage, not as part of the release. The characteristics of the inflow volumes, evaporation rates, area versus storage curves, reservoir losses, and the planned diversion have been described in the previous chapter or are included in Appendix A.

Storage and release variables are constrained to be within certain ranges as follows:

$$\begin{aligned} S_i^{\min}(k) \le S_i(k) \le S_i^{\max}(k) , \\ u_i^{\min}(k) \le u_i(k) \le u_i^{\max}(k) , \\ k = 0,1,\ldots,N . \end{aligned} \tag{3.2}$$

The upper and lower storage limits in (3.2) correspond to the reservoir conservation storage zones reported in the previous chapter. (Flood storage is not included in the controllable storage range because the study uses a monthly time discretization. Namely, this storage is always assumed available to accommodate high frequency hydrologic events.) The lower release limits are constrained by the environmental and water supply requirements. The environmental requirements are constant throughout the year, while water supply requirements change seasonally (Table 2.5). The water diversion amounts to 600 million cubic meters per year. If the control horizon, N, is 12 months, the value of $S_8(12)$ is actually the amount of the annual water transfer. In the simulation studies presented in Chapter 4, the annual water diversion is constrained to be 600 million cubic meters within each hydrologic year, i.e., from October to September. The upper release bounds are determined based on the hydro plant capacity and the specific power generation curves (reported in Chapter 2 and Appendix A).

In view of the inflow uncertainty, storage constraints are more properly expressed in a probabilistic form:

$$
\begin{aligned}
&Prob[S_i^{\min}(k) \le S_i(k)] \ge \pi_i^{\min}(k) \\
&Prob[S_i(k) \le S_i^{\max}(k)] \ge \pi_i^{\max}(k) \\
&i = 1,2,...,7, \quad k = 0,1,...,N,
\end{aligned}
\tag{3.3}
$$

where $\pi^{\min}$ and $\pi^{\max}$ are reliability levels. These levels as well as the upper and lower storage and release thresholds are denoted here as time-varying but are usually time-invariant.

Equations (3.1), (3.2), and (3.3) summarize the reservoir system model. In control systems terminology, reservoir storages are the state variables, and releases are the control variables. The goal of the control algorithm is to identify the release sequences $\{u_i^*(k), i=1,2,...,8; k=0,1,...,N-1\}$ such that system objectives and constraints are met successfully. The element of the formulation that brings this to bear and also measures the success of the various operational alternatives is the performance index which we discuss next.

3.1.2 Performance Index

The control methodology aims at maximizing the benefit of the entire system, while meeting its environmental and water supply demands. To achieve this objective, it minimizes the following performance index:

$$
\begin{aligned}
J = E\{\sum_{k=0}^{N-1} [P_{eng}(u(k),S(k)) + P_h(S(k)) + P_{strg}(S(k)) + P_{utrg}(u(k))] \\
+ P_h(S(N)) + P_{strg}(S(N))\},
\end{aligned}
\tag{3.4}
$$

where

$$
\begin{aligned}
P_{eng}(u(k),S(k)) = -\lambda_p\{\sum_{i=1}^{7} \alpha_i E_{pi}(u_i(k),S_i(k)) + E_{p8}(u_8(k),S_2(k),S_7(k))\} \\
-\lambda_s\{\sum_{i=1}^{7} \alpha_i E_{si}(u_i(k),S_i(k)) + E_{s8}(u_8(k),S_2(k),S_7(k))\},
\end{aligned}
\tag{3.5}
$$

$$P_h(S(k)) = \sum_{i=1}^{7} \beta_{1i} \left[\frac{[H_i^{\max} - H_i(S_i^{\pi_i^{\max}}(k))]^2}{1 + e^{\frac{H_i^{\max} - H_i(S_i^{\pi_i^{\max}}(k))}{T_H}}} + \frac{[H_i(S_i^{\pi_i^{\min}}(k)) - H_i^{\min}]^2}{1 + e^{\frac{H_i(S_i^{\pi_i^{\min}}(k)) - H_i^{\min}}{T_H}}} \right] \quad \textbf{(3.6)}$$

$$P_{strg}(S(k)) = \sum_{i=1}^{7} \gamma_i \left[\frac{H_i(S_i(k)) - H_i^{trg}(k)}{H_i^{\max} - H_i^{\min}} \right]^2 + \gamma_8 [S_8(k) - S_8^{trg}(k)]^2 \quad (3.7)$$

$$P_{utrg}(u(k)) = \sum_{i=1}^{8} \delta_i (u_i(k) - u_i^{trg}(k))^2 \quad (3.8)$$

In (3.4), E{ } denotes expectation of the quantity in the brackets with respect to the joint probability distribution of the reservoir inflows. There are four terms in the performance index. The first term represents the energy value generated from all power facilities in the system including the pumping station. The energy generation consists of two parts: primary and secondary. Primary energy is the energy generated during the peak period of a day, which is herein assumed to last for 6 hours. Typical energy prices are 12 drachma per KWH for the peak hours (λ_p) and 6 drachma per KWH for the off peak hours (λ_s). Sensitivity runs were also conducted for peak to off peak energy prices of 12:4 and 12:8. Pefkofito can be operated in either a generation mode or a pumping mode. When pumping, it consumes secondary energy. $E_{p8}(k)$ and $E_{s8}(k)$ in (3.5) represent the adjusted primary and secondary energy generated from Pefkofito, which are derived as described in Appendix B. The power functions for all other facilities are discussed in the previous chapter, and their corresponding characteristic curves are summarized in Appendix A. The negative signs in (3.5) are introduced to be consistent with a minimization algorithm.

The system benefit also includes the profit generated from irrigation. Typical value of water used in irrigation is 20 drachma per cubic meter. As this value applies *uniformly* over the irrigation season--we have no information on the *relative* value of irrigation at different stages of

the growing season–, maximizing the agriculutral benefit is equivalent to maximizing the April to September release volume from Mouzaki. Mathematically, this is accomplished through the release targets, $P_{utrg}(\mathbf{u}(k)$, as explained below.

The second term is intended to keep reservoir elevations within their respective bounds, $[H^{min}, H^{max}]$. Essentially, if a reservoir level is outside its bounds, term (3.6) imposes a quadratic penalty term is imposed to it.

The third term $P_{strg}(\mathbf{S}(k))$ represents the penalty for the target elevation. For the reservoir state variables, the purpose of this penalty is to force the reservoir elevation to follow a certain target value. In this case, the maximum elevation is assigned as the target value to operate the turbines at high efficiency. This term also improves the convergence speed of the optimization algorithm as discussed later. For the augmented state variable S_8, this term is used to force the cumulative diversion to equal a target value within a certain period.

Similar to the third term, the fourth term $P_{utrg}(\mathbf{u}(k))$ is the penalty for the target release. The purpose of this penalty is to force the reservoir release to follow a certain target value (or pattern). This term is useful if the release target pattern or value is provided. In this application, the target values are calculated dynamically based on the forecasts. For Mouzaki, the release targets for April to September follow the distribution of the irrigation demands, with the highest value (July) is equal to the turbine capacity. Placing the control variable in this quadratic term also improves the convergence speed of the optimization procedure.

Penalty parameters α_i, β_i, γ_i, and δ_i are used to introduce priorities in the performance index terms. In this case, these parameters are determined such that the second term (level constraints) is dominant, followed by the first term (energy value). The third and fourth terms are only present to convexify the optimization problem, except for Mouzaki whose release target is given higher priority. The rationale is to determine feasible sequences (2nd term) guaranteed to maximize the energy and irrigation benefits (1^{st} and 4^{th} terms).

3.2 ELQG Control Method

The control problem formulated in the previous section is solved using the Extended Linear Quadratic Gaussian (ELQG) control method which was originally introduced by *Georgakakos and Marks, 1987,* and further developed by *Georgakakos 1989, 1991, 1993, Georgakakos et al., 1995a, Georgakakos and Yao, 1995,* and *Georgakakos et al., 1997a,b,c.* ELQG is an iterative optimization procedure starting from an initial control sequence {**u**(k); k = 0, 1, 2, .., N-1} and subsequently generating increasingly better sequences until convergence. Convergence is achieved when the value of the performance index cannot be reduced any further. ELQG is reliable, computationally efficient, and especially suited for uncertain, multi- reservoir systems. A short account of the ELQG optimization procedure and features follows next.

The above optimization problem includes three elements: system dynamics, constraints, and performance index. These can be expressed in the following general form:

- System Dynamics:

$$\begin{aligned} \boldsymbol{S}(k+1) &= \boldsymbol{f}[\boldsymbol{S}(k), \boldsymbol{u}(k), \xi(k), k] \\ k &= 0, 1, \ldots, N-1 \ , \end{aligned} \tag{3.9}$$

- Constraints:

These are associated with the system reservoirs and should be expressed in a probabilistic form due to the uncertain system nature.

$$\begin{aligned} & Prob[H_i^{\min}(k) \le H_i(S_i(k))] \ge \pi_i^{\min}(k) \\ & Prob[H_i(S_i(k)) \le H_i^{\max}(k)] \ge \pi_i^{\max}(k) \\ & u_i^{\min}(k) \le u_i(k) \le u_i^{\max}(k) \ , \\ & i = 1, 2 \ldots, 8, \quad k = 0, 1, \ldots, N, \end{aligned} \tag{3.10}$$

- Performance Index:

$$\underset{\boldsymbol{u}(k),\, k=0,1,\ldots,N-1}{Minimize}\ J = E\left\{ \sum_{k=0}^{N-1} g_k[\boldsymbol{S}(k), \boldsymbol{u}(k)] + g_N[\boldsymbol{S}(N)] \right\}, \tag{3.11}$$

where **S**(k), **u**(k), and ξ(k) are the state, control, and uncertain input vectors defined in Section 3.2, π_i^{min} *and* π_i^{max} are reliability parameters, g_k is a function including all performance index terms associated with period k, and g_N is a function including terms associated with the terminal time N. (As before, bold type indicates vector or matrix quantities.)

The Extended Linear Quadratic Gaussian (ELQG) solution procedure starts with an initial control sequence $\{\boldsymbol{u}^0(k),\ k = 0,1,...,N-1\}$ and the corresponding mean state sequence $\{\bar{\boldsymbol{S}}^0(k),\ k = 0,1,...,N\}$:

$$\begin{aligned} \bar{\boldsymbol{S}}^0(k+1) &= \boldsymbol{f}[\bar{\boldsymbol{S}}^0(k), \boldsymbol{u}^0(k), \bar{\xi}(k), k] \\ \bar{\boldsymbol{S}}^0(0) &= \boldsymbol{S}(0) = \textit{known}\ , \\ k &= 0,1,...,N-1\ , \end{aligned} \tag{3.12}$$

where $\bar{\xi}(k)$ represents the mean of the random processes. The next step is to define a perturbation model valid around these nominal state and control sequences. This model describes the dynamic relationship of the state, control, and input vector perturbations,

$$\begin{aligned} \Delta\boldsymbol{S}(k) &= \boldsymbol{S}(k) - \bar{\boldsymbol{S}}^0(k)\ ,\quad k = 0,1,...,N, \\ \Delta\boldsymbol{u}(k) &= \boldsymbol{u}(k) - \boldsymbol{u}^0(k)\ ,\quad k = 0,1,...,N-1, \\ \Delta\xi(k) &= \xi(k) - \bar{\xi}(k)\ ,\quad k = 0,1,...,N-1, \end{aligned} \tag{3.13}$$

and has the following form:

$$\begin{aligned} \Delta\boldsymbol{S}(k+1) &= \boldsymbol{A}(k)\,\Delta\boldsymbol{S}(k) + \boldsymbol{B}(k)\,\Delta\boldsymbol{u}(k) + \boldsymbol{C}(k)\,\Delta\xi(k)\,, \\ \Delta\boldsymbol{S}(0) &= \boldsymbol{0}\,, \\ k &= 0,1,...,N-1\,, \end{aligned} \tag{3.14}$$

where the matrices **A**(k), **B**(k), and **C**(k) represent the gradient matrices of the state transition function with respect to the state, control, and input vectors respectively:

$$A(k) = \nabla_{S(k)} f(k) = \begin{bmatrix} \frac{df_1(k)}{dS(k)} \\ \frac{df_2(k)}{dS(k)} \\ \vdots \\ \frac{df_8(k)}{dS(k)} \end{bmatrix}, \quad B(k) = \nabla_{u(k)} f(k) = \begin{bmatrix} \frac{df_1(k)}{du(k)} \\ \frac{df_2(k)}{du(k)} \\ \vdots \\ \frac{df_8(k)}{du(k)} \end{bmatrix}, \quad C(k) = \nabla_{\xi(k)} f(k) = \begin{bmatrix} \frac{df_1(k)}{d\xi(k)} \\ \frac{df_2(k)}{d\xi(k)} \\ \vdots \\ \frac{df_8(k)}{d\xi(k)} \end{bmatrix}. \tag{3.15}$$

The performance index is also expressed in terms of the perturbation variables as follows:

$$\begin{aligned} J = E\{\sum_{k=0}^{N-1} [\frac{1}{2} \Delta S^T(k)\, Q_{SS}(k)\, \Delta S(k) + q_S{}^T(k)\, \Delta S(k) \\ + \frac{1}{2} \Delta u^T(k)\, R_{uu}(k)\, \Delta u(k) + r_u{}^T(k)\, \Delta u(k) + \Delta u^T(k)\, Q_{uS}(k)\, \Delta S(k)] \\ + \frac{1}{2} \Delta S^T(N)\, Q_{SS}(N)\, \Delta S(N) + q_S{}^T(N)\, \Delta S(N)\}, \end{aligned} \tag{3.16}$$

where $\mathbf{Q}_{ss}(k)$, $\mathbf{q}_s(k)$, $\mathbf{R}_{uu}(k)$, $\mathbf{r}_u(k)$, $\mathbf{Q}_{us}(k)$ are coefficient matrices defining a quadratic approximation of the original performance index. These matrices include the first and second partial derivatives of the $g_k[\ ]$ and $g_N[\ ]$ functions with respect to the state and control variables evaluated at the nominal sequences:

The perturbation control problem defined above is next solved to generate an optimal control sequence $\{\Delta\mathbf{u}^*(k), k=0,1, ..., N-1\}$. This constitutes the optimization direction which defines the new nominal control sequence according to the following relationship:

$$\boldsymbol{u}^{new}(k) = \boldsymbol{u}^{0}(k) + \alpha\, \Delta\boldsymbol{u}^{*}(k)\ , \qquad k = 0,1,\ldots,N-1\ , \tag{3.18}$$

where α is the optimization step size. Some important features of the ELQG solution process are summarized below:

- The ELQG iterations are (**1**) analytically-based (the optimization directions are obtained by Riccati-like equations), (**2**) reliable (the iteration process is guaranteed to converge if the problem has a feasible solution), and (**3**) computationally efficient (convergence is fast). In fact, in the neighborhood of the optimum, it can be theoretically shown that the method converges at a quadratic rate.

- Control constraints are not included in the performance index as penalty terms but are handled *explicitly* through a Projected-Newton procedure. This has important computational efficiency implications as it allows for many constraints to enter or exit the binding control set at the same iteration. The optimization direction is then obtained in the space of the binding constraints.

One last complication is that in order to compute the control gains {D(k), L(k), Λ(k), k=0,1,...,N} one must already have the storage probability distribution. This, however, is resolved by adopting an iterative approach. Namely, the algorithm is first initiated with the Gaussian approximation approach described above, and a set of control gains is computed. Then, the storage traces are generated, and the process is repeated. Based on our experience with the HAD system, in two to three iterations, the probability distributions converge to their true forms and the procedure can terminate.

- State (or, equivalently, elevation) constraints are handled through the barrier penalty

functions discussed in the previous section. This approach has proven to be reliable and computationally efficient. Handling of the state constraints requires the characterization of the state probability density. A two-phase process is used for the state density computation. In the first phase, this density is approximated by its mean and covariance vector, respectively obtained by equations (3.12) and (4.19):

$$\begin{aligned} \boldsymbol{P}_S(k+1) &= \boldsymbol{F}(k)\,\boldsymbol{P}_S(k)\,\boldsymbol{F}^T(k) + \boldsymbol{C}(k)\,\boldsymbol{P}_\xi(k)\,\boldsymbol{C}^T(k)\,, \\ \boldsymbol{F}(k) &= \boldsymbol{A}(k) - \boldsymbol{B}(k)\,\boldsymbol{D}(k)\,\boldsymbol{L}(k)\,, \\ k &= 0,1,\ldots,N-1\,, \end{aligned} \tag{3.19}$$

where $\mathbf{P}_S(k)$ and $\mathbf{P}_\xi(k)$ are the state and input covariance matrices and $\{\mathbf{D}(k), \mathbf{L}(k), k=0,1,\ldots,N-1\}$ are control gains generated by the ELQG solution process. These gains represent a linear approximation of the true feedback laws and are used in the covariance computation to indicate that future decisions will take into consideration measurements of reservoir storage (feedback). The state mean and covariance are then used to construct a normal approximation of the state probability density and convert constraints (3.12) into deterministic equivalents on the elevation mean:

$$\begin{aligned} &\Phi_i^{\min}(k) \le \overline{H}_i(S_i(k)) \le \Phi_i^{\max}(k)\,, \\ &i = 1,2,\ldots,8, \quad k = 0,1,\ldots,N, \end{aligned} \tag{3.20}$$

where $\{\Phi_i^{\min}, \Phi_i^{\max}\}$ are the mean reservoir elevations such that

$$\begin{aligned} &Prob[H_i^{\min}(k) \le H_i(S_i(k))] = \pi_i^{\min}(k)\,, \\ &Prob[H_i(S_i(k)) \le H_i^{\max}(k)] = \pi_i^{\max}(k)\,, \\ &i = 1,2,\ldots,8, \quad k = 0,1,\ldots,N. \end{aligned} \tag{3.21}$$

After the convergence of the first step, the generated control law is then applied to each inflow trace to generate the corresponding storage trace. With the generated storage traces, the

probabilistic characteristics of the state variable are fully defined. The constraints (3.20) and (3.21) are updated. The second phase starts using the recalculated constraints until convergence.

The ELQG iterations continue until the value of the performance index can not be reduced any further. At this point the process terminates, and the current nominal control sequence becomes the problem solution. Under convexity conditions (which are valid in this formulation), this solution is globally optimal. (Convexity can be tested by starting the optimization process from different initial control sequences and verifying that the process converges at the same optimal sequence.)

As mentioned earlier, the control model is applied sequentially, where only the first element of the control sequence is actually applied. The system is then monitored, the new values of the state variables are recorded, and the optimization cycle is repeated at the beginning of the next (decadal) time period. In this way, the model always uses the most updated information regarding the system and continually "tunes" its optimal policies to the current needs and conditions.

More details on the ELQG features can be found in the above-cited references.

CHAPTER 4

CASE STUDIES

4.1 Control Model Runs

In this section, we present some typical results of the control model. This sample run applies to the case of no pumping operation. The water diversion from Sykia to Mouzaki is 600 x 10^6 m^3. The irrigation releases from Mouzaki to the Thessalia region for the irrigation period from April to September are constrained to exceed 600 x 10^6 m^3. These release constraints are distributed according to the irrigation demands of Chapter 2. The length of the control horizon is 12 months starting October 1st. The objective is to maximize the system energy benefit (i.e., the total of primary and secondary energy generation, respectively valued at 12 and 6 drachma per KWh) while meeting the irrigation requirements and avoiding violations of the elevation and other release bounds. The maximum reliability level with which each reservoir can meet its stated constraints varies with the relative magnitude of its storage versus the variability range of its inflows. Thus, in this model run, a reliability of 90% is assigned to Kremasta and Mouzaki; 60% to Mesohora, Sykia, and Pyli; and 50% to Kastraki and Stratos. The minimum release from Stratos (for irrigation and environmental preservation) is 147 million cubic meters per month for May through September and 55.2 million cubic meters per month for the rest of the year. Pyli is also required to release 4 million cubic meters uniformly over the five-month irrigation period. However, this water does not pass through Mouzaki. For the purposes of this model run, the reservoir levels at the beginning of October are taken to be 768 meters at Mesohora, 540 meters at Sykia, 275 meters at Kremasta, 143 meters at Kastraki, 68 meters at Stratos, 335 meters at Pyli, and 285 meters at Mouzaki. Inflow forecasts are generated from a corridor model which generates 20 equally likely inflow traces for each reservoir. This model uses the inflows of the past three months to select historical inflow traces that most closely resemble the current hydrologic situation (in a Euclidian norm sense). All such traces then constitute the forecast ensemble.

Figures C.2.1 through C.2.14 (in Appendix C) show the results of this control model run. The figures respectively depict the traces of reservoir elevation, forecasted inflow, optimal releases, and the associated primary and secondary energy generation amounts. The elevation traces fully satisfy the reliability constraints. The distribution of the water diversion (release sequence of Sykia towards Pefkofito and Mouzaki) are shown in Figure C.2.14. The total diversion amounts to 600 mcm per year. The irrigation requirements for Stratos, Mouzaki, and Pyli are met with the specified reliability.

Table 4.1.1 includes a summary of the expected annual energy generation (primary and secondary), energy value, irrigation volume, and irrigation value by reservoir and for the entire system. The unit price for peak and off-peak energy are taken to be 12 and 6 drachma per KWH respectively, while the value of irrigation is set to 20 drachma per cubic meter.

Table 4.1.1: Annual Expected Energy and Irrigation Statistics

	Expected Primary Energy (GWH) / Value (10^9 drachma)	Expected Secondary Energy (GWH) / Value (10^9 drachma)	Expected Total Energy (GWH) / Value (10^9 drachma)	Expected Irrigation Volume (mcm) / Value (10^9 drachma)
Mesohora	236 / 2.83	127 / 0.76	363 / 3.59	
Sykia	179 / 2.15	192 / 1.15	371 / 3.3	
Kremasta	764 / 9.17	425 / 2.55	1185 / 11.72	
Kastraki	518 / 6.21	187 / 1.12	705 / 7.34	
Stratos	253 / 3.04	106 / 0.64	359 / 3.68	452.5 / 9.05
Pyli				3.5 / 0.07
Mouzaki	270 / 3.24	3 / 0.02	273 / 3.25	680 / 13.59
Pefkofito	235 / 2.82	97 / 0.58	332 / 3.4	
Total	2455 / 29.46	1138 / 6.83	3593 / 36.28	1136 / 22.7

Figures C.2.15 through C.2.22 depict the exceedance probability curves for the annual values of primary energy, secondary energy, and energy value. These curves are useful indicators of the anticipated energy output variability.

In the following section, the control model will be used in sequential control-simulation

experiments to assess the benefits and impacts which accrue from various system configurations and operational scenarios.

4.2 Assessment Investigations

In this section, we discuss the results of several control-simulation experiments, the purpose of which is to quantify the performance of different system configurations and operational scenarios.

The basis of the control-simulation experiments presented herein is the 32-year long monthly historical inflow record (1961-1993) which is shown on Figures C.3.1, C.3.2, and C.3.3 in Appendix C. The control-simulation process is as follows: For each month of the historical record, the control model is activated first to generate the optimal reservoir release sequences. The control model is implemented with a 12-month control horizon, inflow forecasts generated by the corridor forecasting model, and a reliability level of 50%. The values of the reservoir elevations for each month of the simulation are determined based on the results of the previous step, while at the very start of the simulation, they are taken to be 768 meters at Mesohora, 540 meters at Sykia, 275 meters at Kremasta, 143 meters at Kastraki, 68 meters at Stratos, 335 meters at Pyli, and 285 meters at Mouzaki. From the 12-month optimal release sequences, only the first month's optimal releases are actually implemented, and the system response is simulated using the historically observed inflows (not known at the time of the forecast). If the optimal releases result in feasible end-of-the-month reservoir elevations, the program completes this control-simulation step, records these elevations along with the releases and the energy generation amounts, and repeats this process at the next month. Otherwise, appropriate release adjustments are made so that all reservoirs stay within their feasible ranges. This control-simulation process is repeated for 384 (= 32 x 12) months and results in a long series of simulated reservoir elevations, releases, irrigation deficits, and energy generation amounts. This data series is then analyzed to develop statistics of system performance and make comparisons.

Figure 4.2.1 depicts the conceptual organization of the assessment investigations. We start with the results for system configuration A which includes Kremasta, Kastraki, and Stratos. We next investigate system B which *additionally* includes the reservoirs and hydropower facilities of Mesohora and Sykia (five reservoirs in all). After that, we consider system C which also includes the diversion, the hydropower facility at Pefkofito with no pump-back operation,

and Mouzaki. The next configuration is system D which is essentially the same as system C with the *added* option of pumping water from Mouzaki to Sykia through the reversible turbines at Pefkofito. The last configuration is system E which is system D expanded to include Pyli (seven reservoirs in all).

Figure 4.2.2 summarizes the results for system configuration A (consisting of Kremasta, Kastraki, and Stratos). The figure includes information on hydropower as well as irrigation. Relative to hydropower, the figure contains frequency curves for the annual primary energy generation, secondary energy generation, and total energy generation. For example, the primary energy graph of the figure indicates that the energy amount of 1500 GWh is exceeded almost 80% of the time, or in 25 out of the 32 years of the simulation. The same graph also indicates that the system produces at least 1200 GWh of primary energy in every year of the 1961-1993 hydrologic period. In addition to the frequency curves, the figure also reports the *average* annual energy amounts (primary, secondary, and total) and their value. Thus, on the average (namely, at the 50^{th} percentile of the frequency curves), this system produces 1569 GWh of primary energy, 719 GWh of secondary energy, and 2,288 GWh of total energy. At prices of 12 drachmas per primary KWh and 6 drachmas per secondary KWh, these energy amounts are valued at 18.82, 4.31, and 23.14 billion drachma per year.

On the irrigation side, we report the irrigation releases at Stratos, Mouzaki, and Pyli. Since Mouzaki and Pyli are not assumed to exist in this configuration, the irrigation amounts at these locations are computed by adding the streamflow values from April to September. At Pyli and Stratos, maximum irrigation water use is restricted to 4 and 462.67 million cubic meters per year respectively. Flows in excess of these amounts do not yield irrigation benefits. At a nominal price of 20 drachma per cubic meter, the value of water provided to irrigation is 10.07 billion drachma annually. Thus, under the assumptions stated earlier, the economic gains from the two major water uses (hydropower and irrigation) are significantly different, with irrigation valued less than half relative to hydropower. The total value of water from hydropower *and* irrigation is about 33.21 billion drachma per year. The last item reported on the figure indicates the extent to which the system is depleted and is expressed by the sum total of the *active* storage volume left in the system reservoirs at the end of the simulation horizon. In this model run, this

total volume is 1,547.46 million cubic meters which approximately represents 43% of the system active storage capacity (3,561 million cubic meters).

More detailed results for each system reservoir and time period can be found in the extensive tables and figures in Appendix C. These results include the simulated monthly sequences of reservoir elevation, release, primary and secondary energy generation, and the associated annual exceedance frequency curves. It is clear from these graphs (C.3.4, C.3.5, and C.3.6) that Kremasta is the main storage and regulation project of the Acheloos system. Thus, the model policy is to keep Kremasta as full as possible (to maximize long-term energy generation efficiency), except during droughts when its storage is used to supplement th inflow process and provide the water necessary for the irrigation demand at Stratos (middle graph on Figure C.3.6) and for the generation of energy. Relative to the latter, this policy also serves to maintain high net heads on the plant turbines and, for the most part, generate dependable peak energy. Secondary energy is produced mainly during wet periods, or when it helps to increase the total energy value without compromising the future generation of primary energy.

Though we will continue to refer to the figures in Appendix C as we proceed with the analysis of the assessment runs, we will use the format of Figure 4.2.2 as our primary means to compare the performance of the various system configurations.

The results for system configuration B (consisting of Mesohora, Sykia, Kremasta, Kastraki, and Stratos) are shown on Figure 4.2.3 together with those of system A. All energy curves show a significant increase due to the contribution of the power stations at Mesohora and Sykia. On average, primary energy is increased by 450 GWh per year (29%), secondary energy by 383 GWh per year (53%), and total energy by 832 GWh per year (36%). The increase of the primary energy is approximately similar over the entire range of the frequency curve, which implies that the system is now guaranteed to generate at least 1,650 GWh in every year of the historical horizon. These increases translate into an economic gain of 7.7 billion drachma annually (33%), 5.4 billion of which is due to primary energy.

The irrigation statistics are identical to those of system A. Thus in this system, the economic value of hydropower exceeds that of irrigation by about 21 billion drachma per year. The total economic value of both water uses amounts to 41 billion drachma per year, which

represents an increase of 8 billion drachma over the previous case. The detailed simulation sequences for this run are shown in Figures C.3.11 through C.3.21.

Figure 4.2.4 additionally includes the statistics for system configuration C (consisting of Mesohora, Sykia, Kremasta, Kastraki, Stratos, and Mouzaki together with the diversion structure and the power plant at Pefkofito). At any given year, the total water transfer from Sykia to Mouzaki is 600 million cubic meters, while no pumping is permitted. Concerning hydropower, the main effect of the water transfer is to enable the generation of more primary energy. Thus on average, primary energy increases by 261 GWh over the generation of system B, while secondary energy decreases by 300 GWh. The result is a net economic gain of about 1.3 billion drachma per year. However, the economic gain with respect to irrigation is much higher. This system configuration guarantees the annual availability of 600 million cubic meters of irrigation water to Thessalia, more than doubling the value of irrigation water use (to 22.83 billion drachma per year). Thus, the diversion is beneficial for both hydropower and irrigation alike, and the total economic gain increases to 55 billion drachma per year.

The simulation sequences for this run are shown in Figures C.3.22 through C.3.36. Comparing Figures C.3.13 and C.3.24 (as well as C.3.18 and C.3.31), we note that the main effect of the diversion on the lower Acheloos system is to reduce secondary energy generation. Primary energy is also affected, especially during the drought of 1988-1993 (tail of the frequency distribution), while no irrigation deficits take place. However, in a system-wide context, these reductions are more than compensated by the energy generation at Pefkofito and Mouzaki.

Figure 4.2.5 assesses the effect of pump-storage operations on system configuration C. This mode of operation affects only hydropower as the net water transfer from Sykia to Mouzaki is the same as before. Primary energy increases even more under this scenario (by about 230 GWh/year on the average), while secondary energy decreases (by about 342 GWh) to make this possible. The average net economic gain of the pumping operations at Pefkofito amounts to 0.71 billion drachma per year, while the irrigation gains remain practically the same. The total economic value of water use is estimated at 55.75 billion drachma per year. As shown by the detailed simulation sequences, pump-storage mainly affects the distribution of energy generation at Pefkofito (compare Figures C.3.28 and C.3.43), which now operates throughout the peak

generation period.

Lastly, Figure 4.2.6 examines the effect of Pyli on the performance of the overall system. Pyli is a relatively small reservoir with an active storage of 46 million cubic meters and no hydropower facilities. Its main contribution is to ensure that Mouzaki has enough water to satisfy its irrigation demand without experiencing severe drawdowns. Furthermore, its releases eventually pass through the Mouzaki hydropower facility and generate additional energy. The results of Figure 4.2.6 show that Pyli enhances the performance of the system on both counts. Total energy generation increases by about 41 GWh per year, of which 39 GWh are due to primary energy increases. The associated economic gain is 0.5 billion drachma per year. Relative to irrigation, Pyli guarantees more irrigation water for Thessalia–the releases from Mouzaki during April to September increase by about 60 million cubic meters per year–resulting in an estimated economic gain (from irrigated agriculture) of 1.2 billion drachma annually. The total value of all water uses is now estimated at 57.44 billion drachma, exceeding all previous scenarios. Pyli also increases the end-storage of the system thus providing added insurance against severe droughts.

There are three more sets of model runs we wish to discuss. These are depicted on Figures 4.2.7, 4.2.8, and 4.2.9 and assess the sensitivity of system E relative to the diversion amount, the price ratio of the primary to secondary energy, and the accuracy of forecasting.

The results in Figure 4.2.7 are obtained by increasing the diversion amount from 500 to 600 to 700 million cubic meters per year. The main difference in the results pertains to the irrigation benefits which increase by about 1.5 billion drachma per year by each additional increase of the diversion amount. Total energy generation and value remain virtually unchanged. The only noteworthy change in this regard is that the amount of primary energy which is guaranteed 100% of the time (firm energy) is 200 GWh higher in the 500 mcm versus the 700 mcm diversion case.

Figure 4.2.8 examines the sensitivity of the system to the price ratio of primary versus secondary energy. Results are shown for the 12:4, 12:6, and 12:8 price ratios. As a general rule, as the price of secondary energy increases relative to the price of the primary energy, secondary energy generation increases and primary generation decreases. The net economic gain depends

on the actual prices. It is also expected that beyond a certain point (not reached in these runs), the pumping operation will become uneconomical.

The last figure compares the results of two runs with forecasting schemes of different accuracy. In fact, the new forecasting scheme is assumed to have perfect foresight of the upcoming 12-month streamflows. The total hydropower and irrigation statistics are similar in the two cases with the corridor forecasting scheme yielding slightly higher economic gains. However, the perfect forecast scheme results in considerably more end system storage. This difference is 1, 368 million cubic meters and can sustain the system's irrigation requirements for more than a year. In this sense, it would be valued at about 26 billion drachma which could be annualized to about 0.8 billion drachma per year. The same storage represents about 30% of the annual system inflow volume and has value relative to energy generation as well. Thus, the hydropower value of the extra storage could roughly be estimated at 10 billion drachma, or 310 million drachma per year. To be sure, perfect forecasting is not attainable. However, this comparison does provide an upper bound for the value of forecasting. Figures C.3.68 through C.3.83 show the monthly sequences and statistics that would result under a perfect forecast scenario. With such foresight, the model manages to maintain high reservoir levels and minimize the range of reservoir fluctuation.

The previous assessments are valid provided that the system is managed by the control model developed herein. Namely, the various system configurations may fail to achieve the indicated performance if reservoirs are regulated by some heuristic or sub-optimal approach (such as the commonly used reservoir rule curves).

Lastly, the magnitude of the economic gains pertaining to each system configuration is sensitive to the prices used for the value of energy generation and irrigation usage. From this standpoint, emphasis should be placed on *relative* and not *absolute* performance. Thus, if future studies suggest other unit prices, the previous investigations should be repeated and the conclusions be revisited. The decision software is designed to facilitate such efforts.

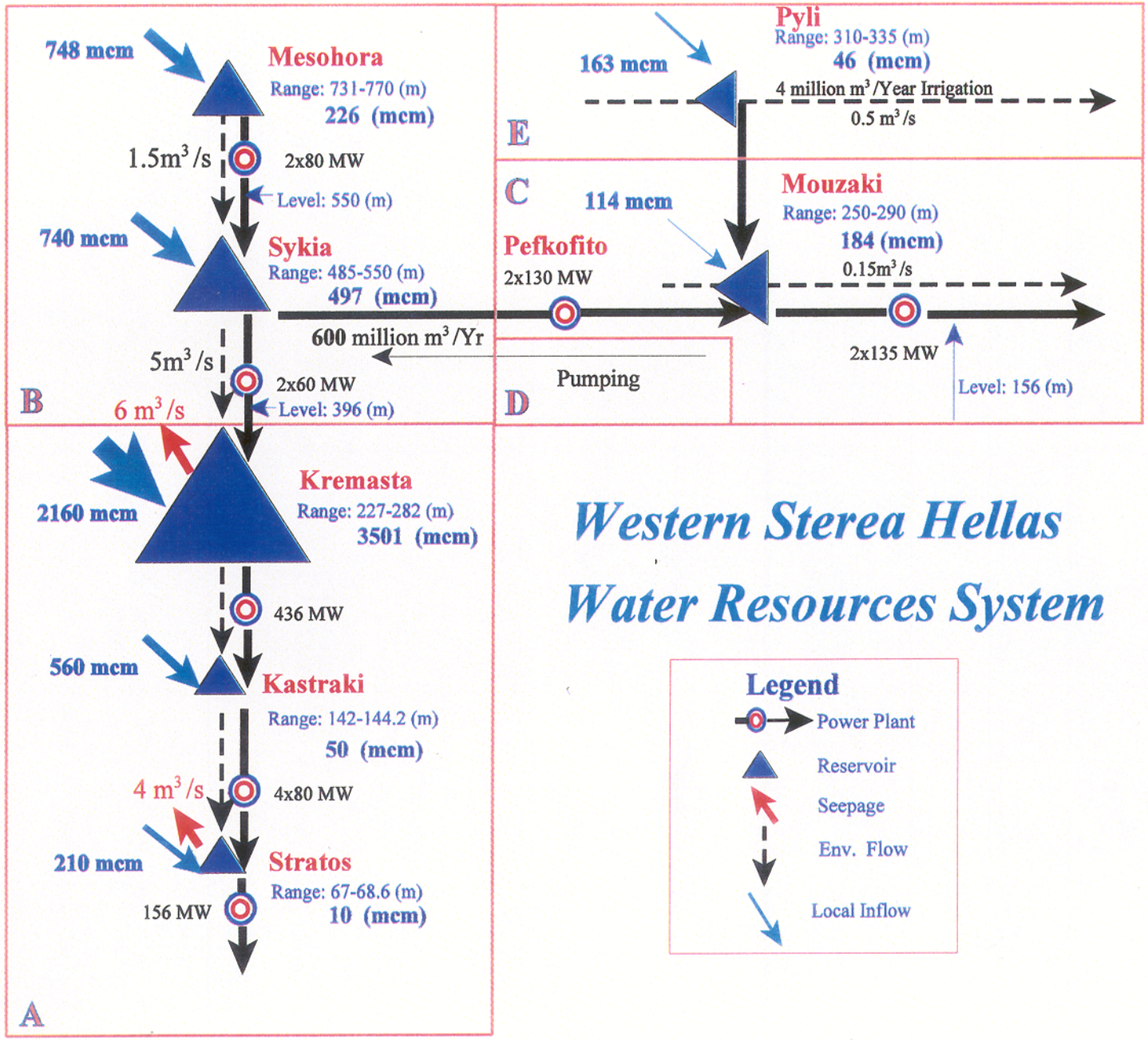

Figure 4.2.1: System Configurations for Schematic

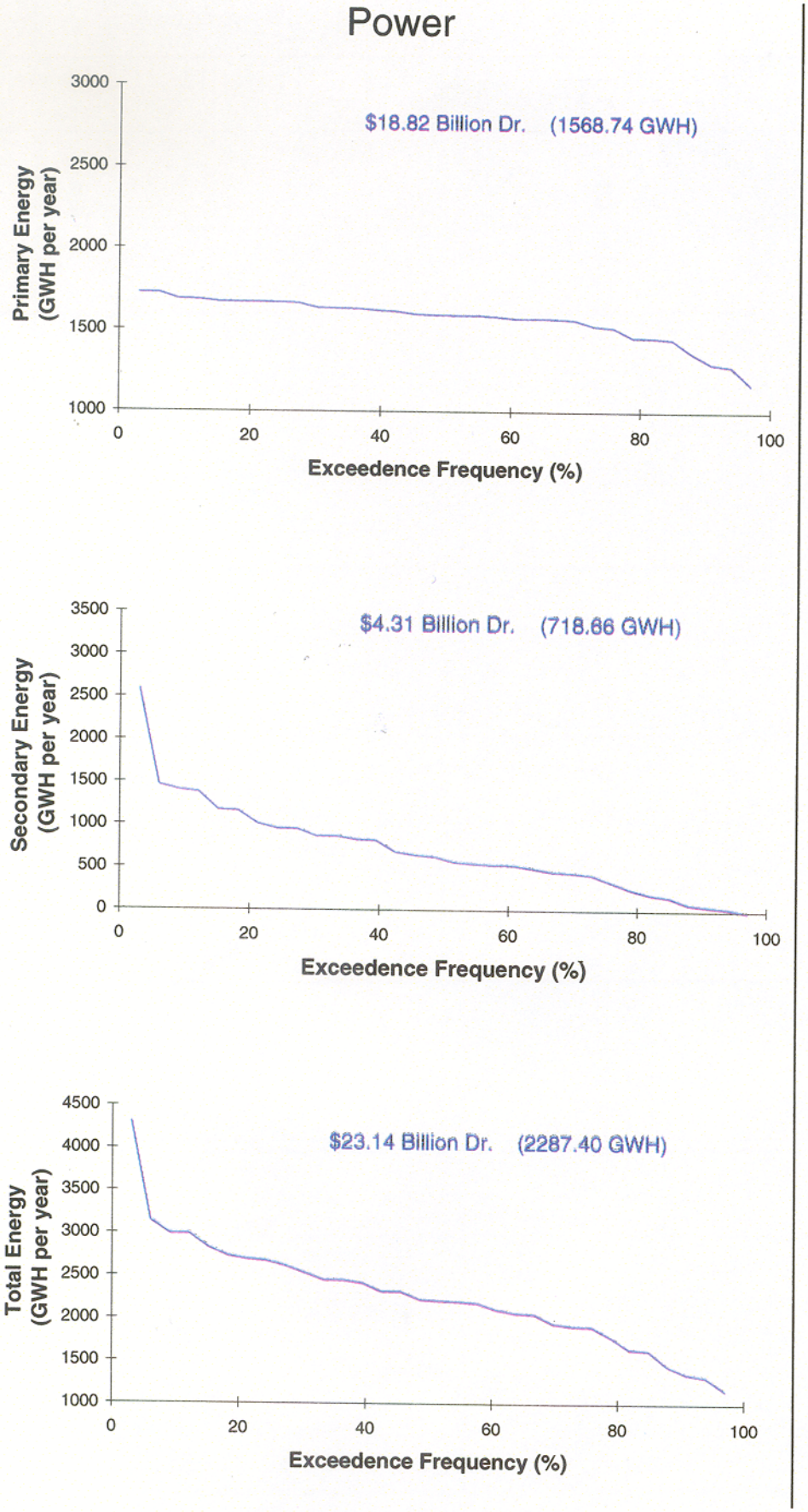

Figure 4.2.2: Summary of Results for System Configuration A.

Power

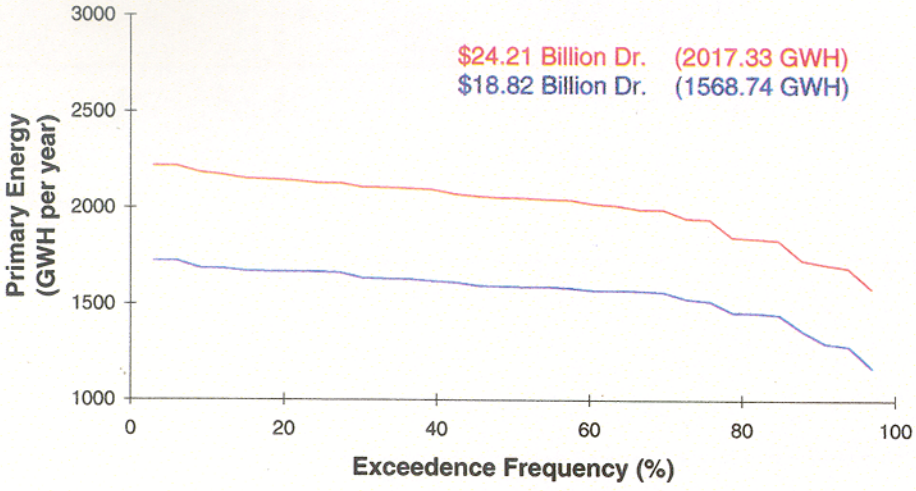

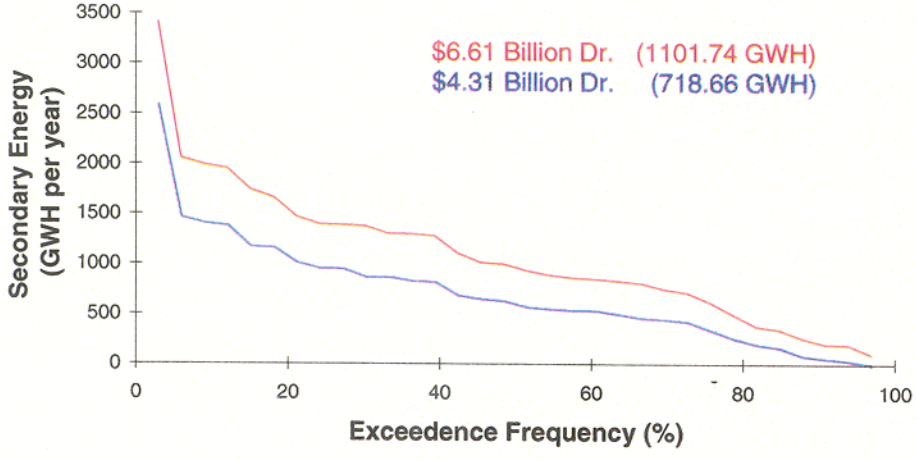

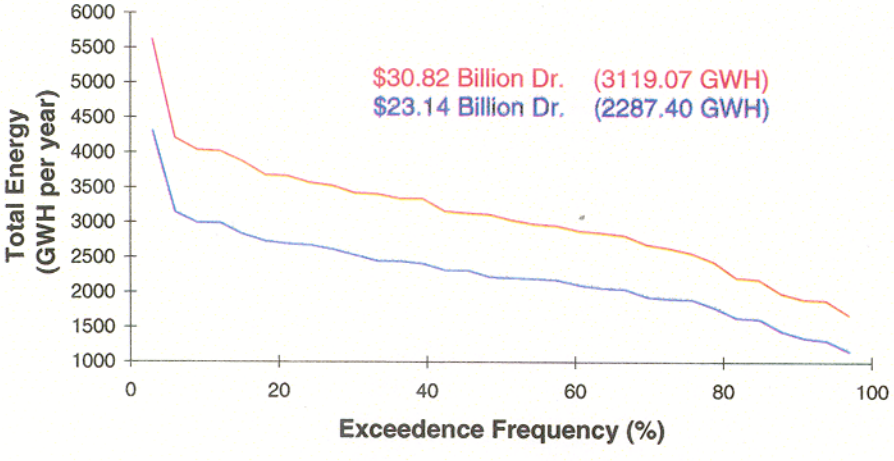

Irrigation

Strts: 462.67 mcm
Mzk: 36.78 mcm
Pl: 4.00 mcm
Total: 503.45 mcm
Value: $10.07 Billion Dr.

B: Mshr-Sk-Krmst-Kstrk-Strts
Storage = 2142.93 mcm

Strts: 462.67 mcm
Mzk: 36.78 mcm
Pl: 4.00 mcm
Total: 503.45 mcm
Value: $10.07 Billion Dr.

A: Krmst-Kstrk-Strts
Storage = 1547.46 mcm

Figure 4.2.3: Summary of Results for System Configurations A, B.

Power

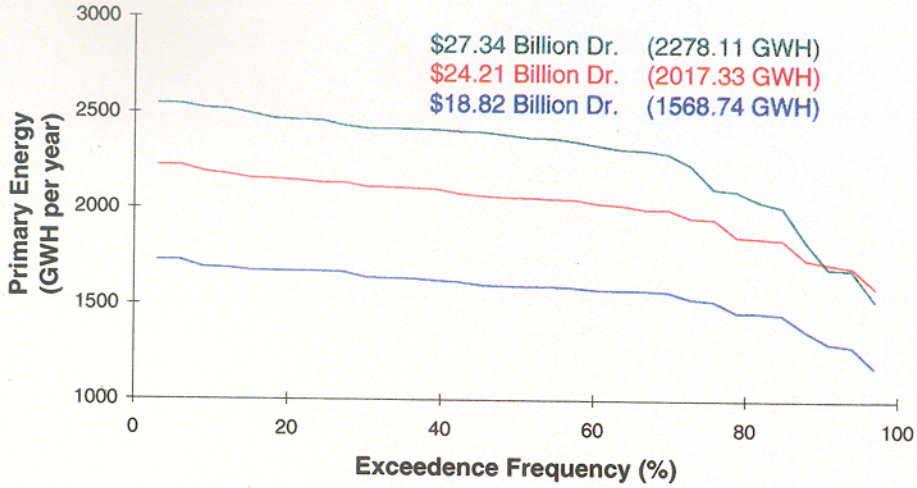

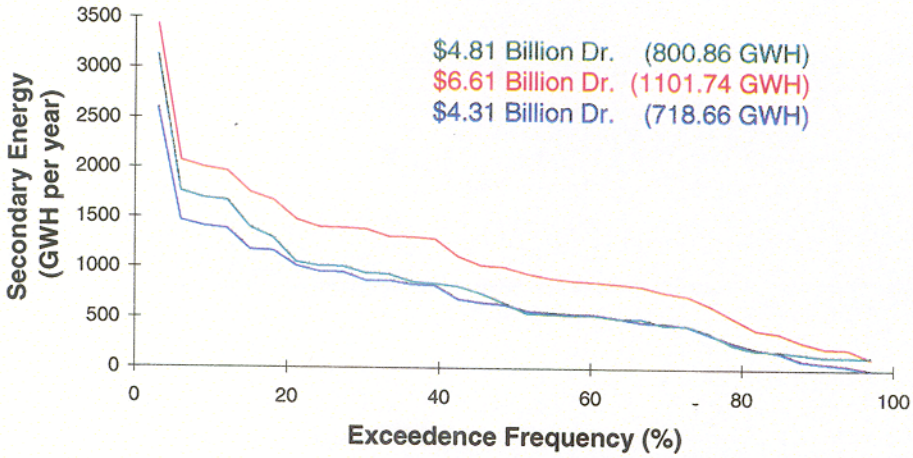

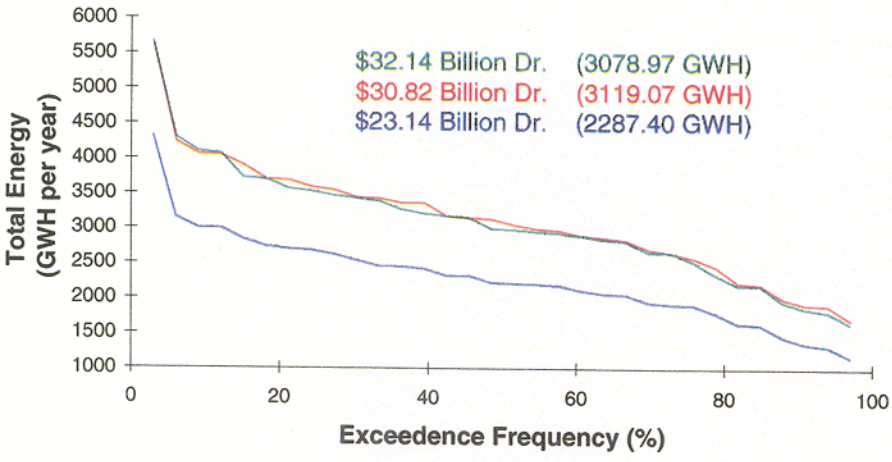

Irrigation

Strts:	462.63 mcm
Mzk:	675.04 mcm
Pl:	4.00 mcm
Total:	1141.67 mcm
Value:	$22.83 Billion Dr.

C: Mshr-Sk-Krmst-Kstrk-Strts-Mzk

Storage = 1648.05 mcm

Strts:	462.67 mcm
Mzk:	36.78 mcm
Pl:	4.00 mcm
Total:	503.45 mcm
Value:	$10.07 Billion Dr.

B: Mshr-Sk-Krmst-Kstrk-Strts

Storage = 2142.93 mcm

Strts:	462.67 mcm
Mzk:	36.78 mcm
Pl:	4.00 mcm
Total:	503.45 mcm
Value:	$10.07 Billion Dr.

A: Krmst-Kstrk-Strts

Storage = 1547.46 mcm

Figure 4.2.4: Summary of Results for System Configurations A, B, C.

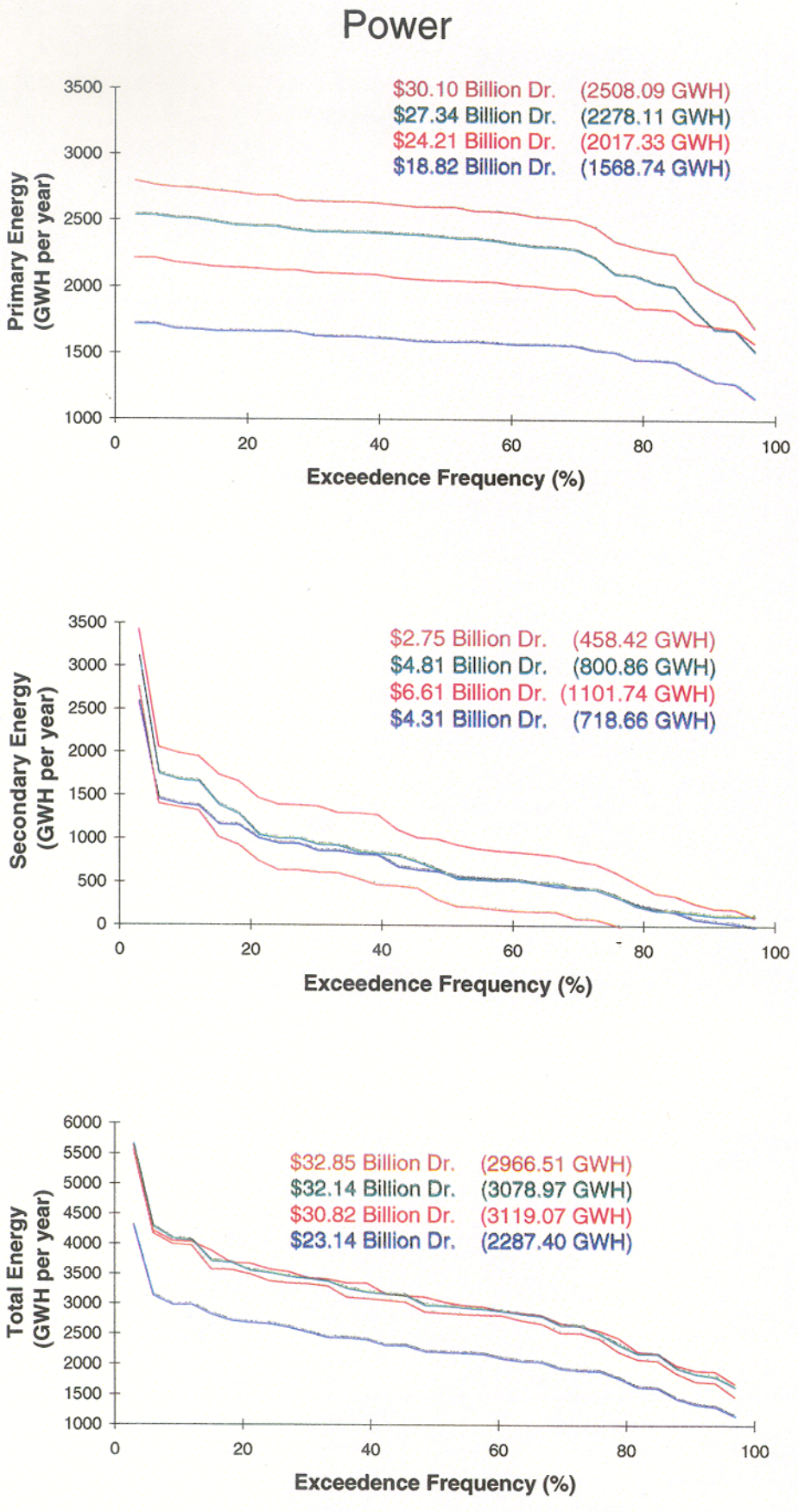

Figure 4.2.5: Summary of Results for System Configurations A, B, C, D.

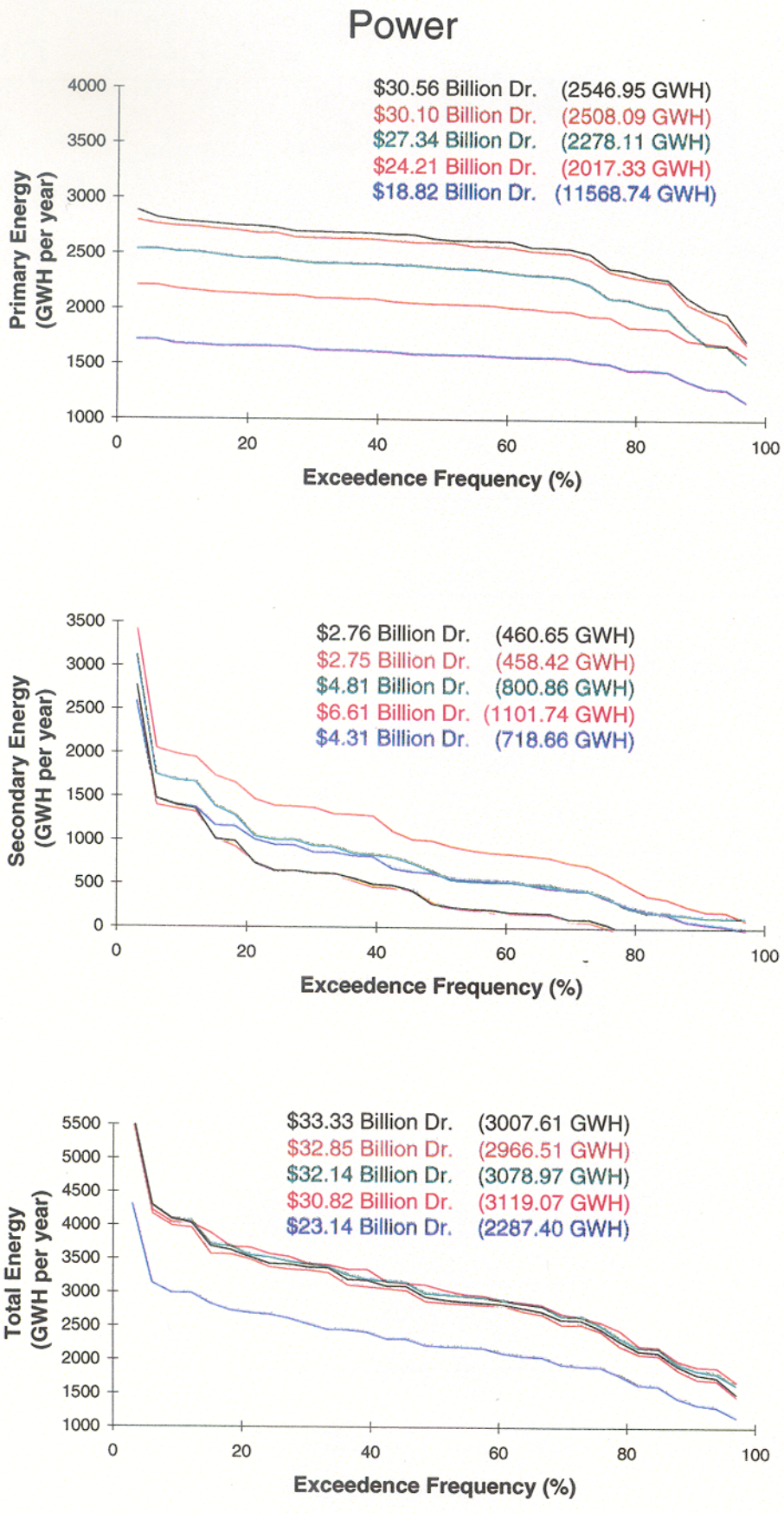

Irrigation

Strts: 462.60 mcm
Mzk: 739.13 mcm
Pl: 4.00 mcm
Total: 1205.73 mcm
Value: $24.11 Billion Dr.

E: Mshr-Sk-Krmst-Kstrk-Strts-Mzk-Pmp-Pl
Storage = 1699.68 mcm

Strts: 462.67 mcm
Mzk: 678.56 mcm
Pl: 4.00 mcm
Total: 1145.23 mcm
Value: $22.90 Billion Dr.

D: Mshr-Sk-Krmst-Kstrk-Strts-Mzk-Pmp
Storage = 1640.75 mcm

Strts: 462.63 mcm
Mzk: 675.04 mcm
Pl: 4.00 mcm
Total: 1141.67 mcm
Value: $22.83 Billion Dr.

C: Mshr-Sk-Krmst-Kstrk-Strts-Mzk
Storage = 1648.05 mcm

Strts: 462.67 mcm
Mzk: 36.78 mcm
Pl: 4.00 mcm
Total: 503.45 mcm
Value: $10.07 Billion Dr.

B: Mshr-Sk-Krmst-Kstrk-Strts
Storage = 2142.93 mcm

Strts: 462.67 mcm
Mzk: 36.78 mcm
Pl: 4.00 mcm
Total: 503.45 mcm
Value: $10.07 Billion Dr.

A: Krmst-Kstrk-Strts
Storage = 1547.46 mcm

Figure 4.2.6: Summary of Results for System Configurations A, B, C, D, E.

Power

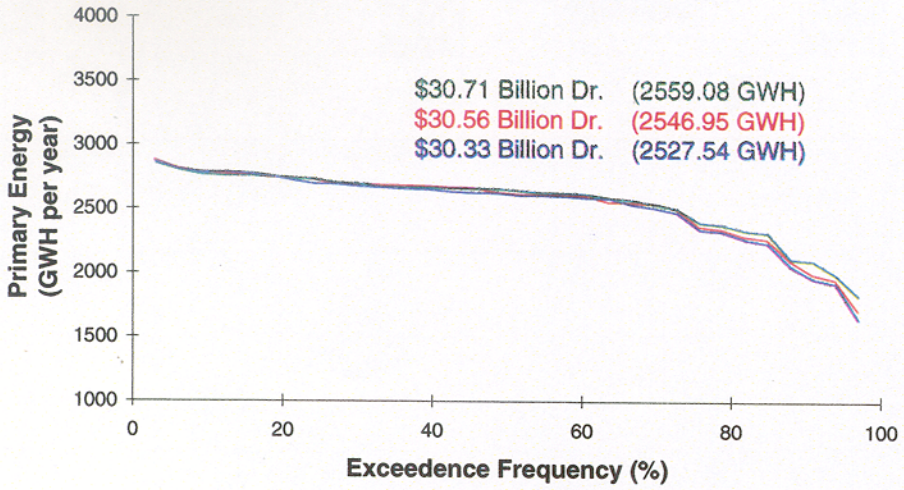

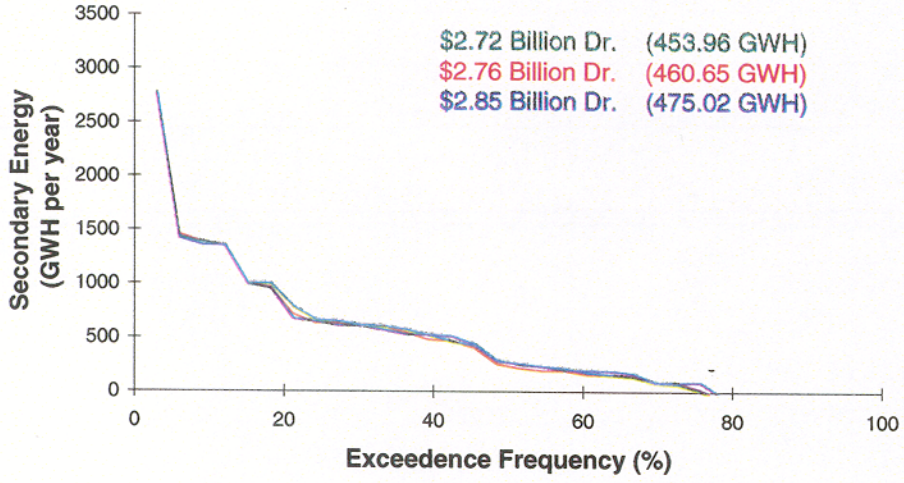

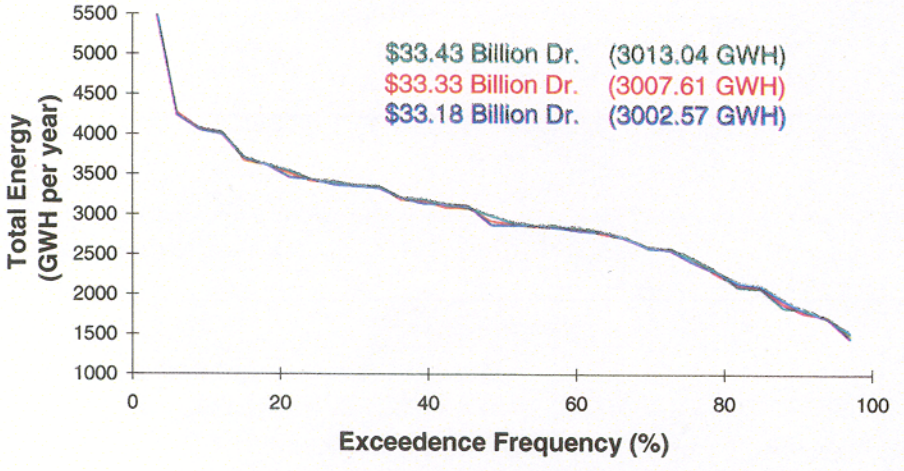

Irrigation

Strts:	462.67 mcm
Mzk:	649.92 mcm
Pl:	3.96 mcm
Total:	1116.55 mcm
Value:	$22.33 Billion Dr.

E: Mshr-Sk-Krmst-Kstrk-Strts-Mzk-Pmp-Pl

Storage =	1797.58 mcm
Diversion =	**500.00 mcm**

Strts:	462.60 mcm
Mzk:	739.13 mcm
Pl:	4.00 mcm
Total:	1205.73 mcm
Value:	$24.11 Billion Dr.

E: Mshr-Sk-Krmst-Kstrk-Strts-Mzk-Pmp-Pl

Storage =	1699.68 mcm
Diversion =	**600.00 mcm**

Strts:	462.67 mcm
Mzk:	802.22 mcm
Pl:	3.99 mcm
Total:	1268.88 mcm
Value:	$25.38 Billion Dr.

E: Mshr-Sk-Krmst-Kstrk-Strts-Mzk-Pmp-Pl

Storage =	1628.19 mcm
Diversion =	**700.00 mcm**

Figure 4.2.7: Sensitivity With Respect to the Diversion Amount (System E).

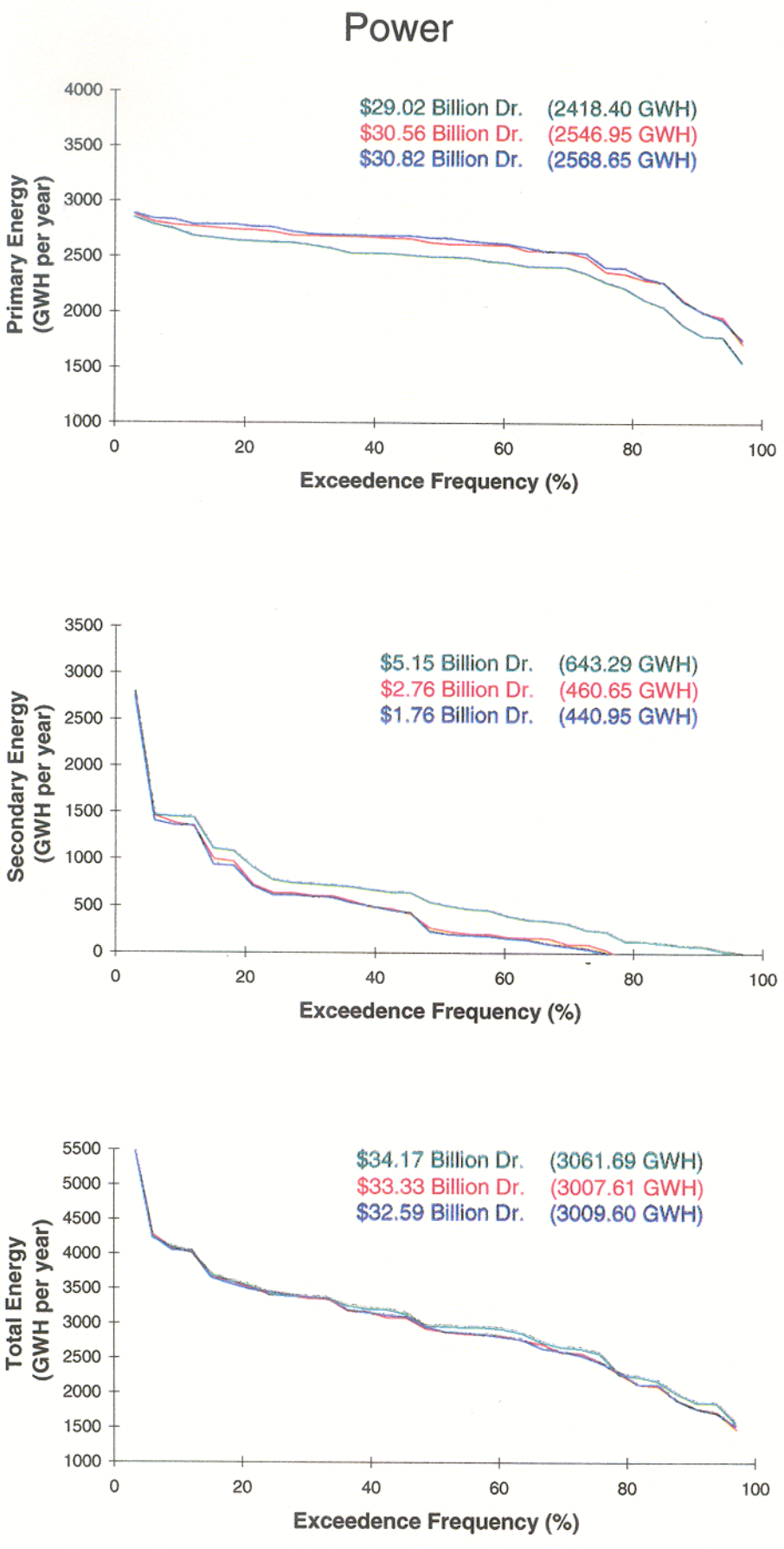

Figure 4.2.8: Sensitivity With Respect to Energy Prices (System E).

Power

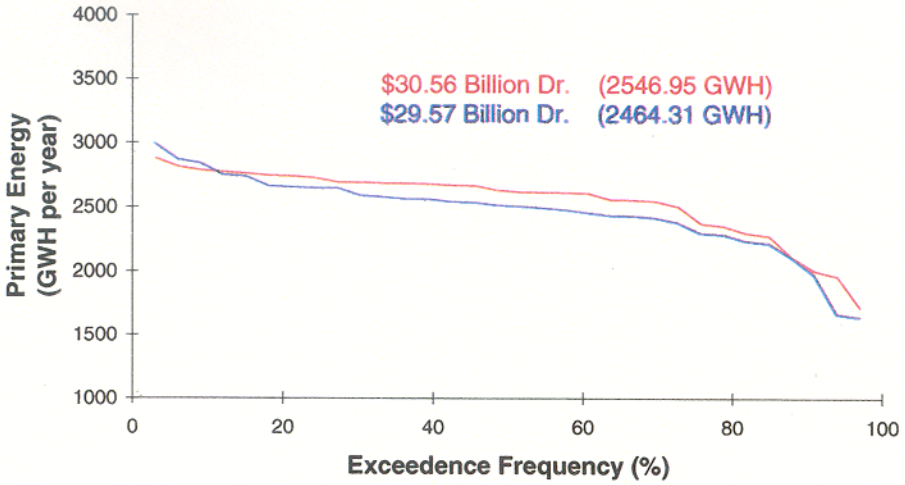

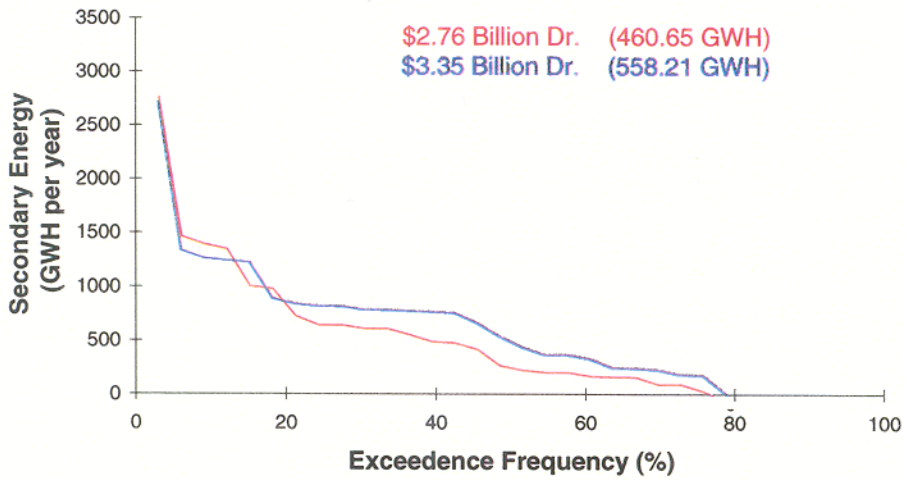

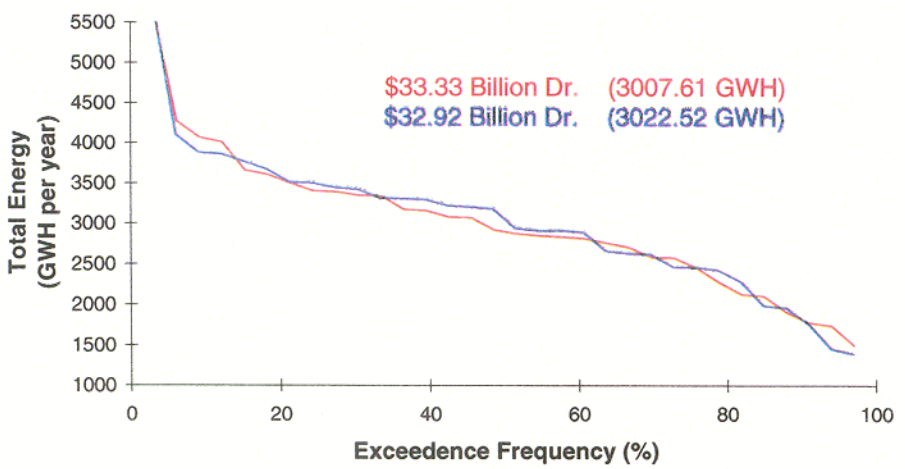

Irrigation

Strts:	462.60 mcm
Mzk:	739.13 mcm
Pl:	4.00 mcm
Total:	1205.73 mcm
Value:	$24.11 Billion Dr.

E: Mshr-Sk-Krmst-Kstrk-Strts-Mzk-Pmp-Pl

Storage = 1699.68 mcm

Corridor Model Forecast

Strts:	462.67 mcm
Mzk:	726.77 mcm
Pl:	4.00 mcm
Total:	1193.44 mcm
Value:	$23.87 Billion Dr.

E: Mshr-Sk-Krmst-Kstrk-Strts-Mzk-Pmp-Pl

Storage = 3067.99 mcm

Perfect Forecast

Figure 4.2.9: Sensitivity With Respect to Forecast Accuracy (System E).

CHAPTER 5

CONCLUSION

The work effort described herein makes technical contributions in two areas: The first area is in the development of a decision model for the planning and management of the Western Sterea Hellas reservoir system. The second, is in the use of this model to assess the impacts of the proposed water diversion and the benefits associated with various system configurations .

The reservoir control model is based on recent advances in reservoir control and circumvents the well-known "dimensionality" limitations. The approach represents all system reservoirs and hydropower facilities in a detailed fashion, incorporates their operational modes (both conventional and pumping) and water use requirements, and develops feedback policies that optimize the system in a fully uncertain framework.

To assess the impacts of the water transfer from the Acheloos Basin to the Thessalia Region, a forecast-control-simulation model was also developed and is a part of the decision support system. Noteworthy findings of the investigations described herein (Chapter 4, Section 4.2) are as follows: (References to the system configurations pertain to Figure 4.2.1)

- On the average the existing reservoir system consisting of Kremasta, Kastraki, and Stratos (system configuration A) produces 1568 GWh of primary energy, 718 GWh of secondary energy, and 2,287 GWh of total energy. At prices of 12 drachmas per primary KWh and 6 drachmas per secondary KWh, these energy amounts are valued at 18.82, 4.31, and 23.14 billion drachma per year. Furthermore, at a nominal price of 20 drachma per cubic meter, the value of water provided to irrigation is 10.07 billion drachma annually. Thus, under the assumptions stated earlier, the economic gains from the two major water uses (hydropower and irrigation) are significantly different, with irrigation valued less than half relative to hydropower.

- The results for system configuration B (consisting of Mesohora, Sykia, Kremasta, Kastraki, and Stratos) show significant energy increases due to the contribution of the power stations at Mesohora and Sykia. On average, primary energy is increased by 450 GWh per year (29%), secondary energy by 383 GWh per year (53%), and total energy by 832 GWh per year (36%). These increases translate into an economic gain of 7.7 billion drachma annually (33%). The irrigation statistics are identical to those of system A.

- System configuration C (consisting of Mesohora, Sykia, Kremasta, Kastraki, Stratos, and Mouzaki together with the diversion structure and the power plant at Pefkofito) entails additional benefits. An average of 261 GWh primary energy increase takes place over the generation of system B, while secondary energy decreases by 300 GWh. The result is a net economic gain of about 1.3 billion drachma per year. However, the economic gain with respect to irrigation is much higher. This system configuration guarantees the annual availability of 600 million cubic meters of irrigation water to Thessalia, more than doubling the value of irrigation water use (to 22.83 billion drachma per year). Thus, the diversion is beneficial for hydropower and irrigation alike.

- The effect of pump-back operations is assessed via system configuration D. This mode of operation affects only hydropower as the net water transfer from Sykia to Mouzaki is the same as before. Primary energy increases even more under this scenario (by about 230 GWh/year on the average), while secondary energy decreases (by about 342 GWh) to make this possible. The average net economic gain of the pumping operations at Pefkofito amounts to 0.71 billion drachma per year.

- Lastly, the incremental effect of Pyli on the performance of the overall system is assessed via system configuration E. Pyli enhances the performance of the system both with respect to hydropower as well as irrigation. Total energy generation increases by about 41 GWh per year, while the associated economic gain is 0.5 billion drachma per year. Relative to irrigation, Pyli guarantees more irrigation water for Thessalia–the releases

from Mouzaki during April to September increase by about 60 million cubic meters per year–resulting in an estimated economic gain (from irrigated agriculture) of 1.2 billion drachma annually. The total value of all water uses is now estimated at 57.44 billion drachma, exceeding all previous scenarios. Pyli also provides added insurance against severe droughts.

- Increasing the diversion amount from 500 to 600 to 700 million cubic meters per year results in increases of the irrigation benefits by about 1.5 billion drachma per year for each additional increase of the diversion amount. Total energy generation and value remain virtually unchanged. The only noteworthy change in this regard is that the amount of primary energy which is guaranteed 100% of the time (firm energy) is 200 GWh higher in the 500 mcm versus the 700 mcm diversion case.

- As the price of secondary energy increases relative to the price of the primary energy, secondary energy generation increases and primary generation decreases. The net economic gain depends on the actual prices. Beyond a certain ratio, the pumping operation becomes uneconomical.

- Comparing the previous runs with a case of perfect forecasting, we found that the hydropower and irrigation statistics are comparable. However, the perfect forecast scheme results in considerably more active system storage. The value of the extra storage is significant and can be estimated at 26 billion drachma relative to irrigation and 10 billion drachma relative to hydropower.

- The previous assessments are valid provided that the system is managed by the control model developed herein. Namely, the various system configurations may fail to achieve the indicated performance if reservoirs are regulated by some heuristic or sub-optimal approach (such as the commonly used reservoir rule curves).

- The magnitude of the economic gains pertaining to each system configuration is sensitive to the prices used for the value of energy generation and irrigation usage. From this standpoint, emphasis should be placed on *relative* and not *absolute* performance. Thus, if future studies suggest other unit prices, the previous investigations should be repeated and the conclusions be revisited. The decision software is designed to facilitate such investigations.

Under the previous caveats, Figure 5.1 summarizes the annual economic gains associated with each system configuration (A, B, C, D, and E) and water use (irrigation, hydropower, and total), and assesses the relative significance of each new system element. The performance levels associated with system configuration E (which includes all elements) are highest and serve as comparison standards. The performance levels of the other configurations are measured as percentages of the optimal levels. The figure shows that expanding the system by constructing Mesohora, Sykia, the diversion, and Mouzaki leads to significant gains which come to within 5% of the optimal levels. And, though pump-storage at Pefkofito and the construction of Pyli add value to the system, these gains are relatively smaller.

The decision system can be enhanced and utilized in several other ways. First, additional information is needed to better represent the hydropower facilities on the Pamisos River. For example, the assumption made here is that the tailrace at Pefkofito is controlled by the Mouzaki reservoir level. Furthermore, downstream of Mouzaki there are two proposed hydropower stations, one at the exit of the Mouzaki reservoir and another at Mavromation. However, no information is available for the latter, and no attempt was made here to model it. Also, the pumping possibility at the Mouzaki hydropower station require more detailed knowledge of the downstream impoundments. However, the situation may change if the facility characteristics are modeled in more detail.

Lastly, the decision system developed herein can easily be expanded to include operational decision models which would aim at refining the monthly release decisions into daily and hourly sequences.

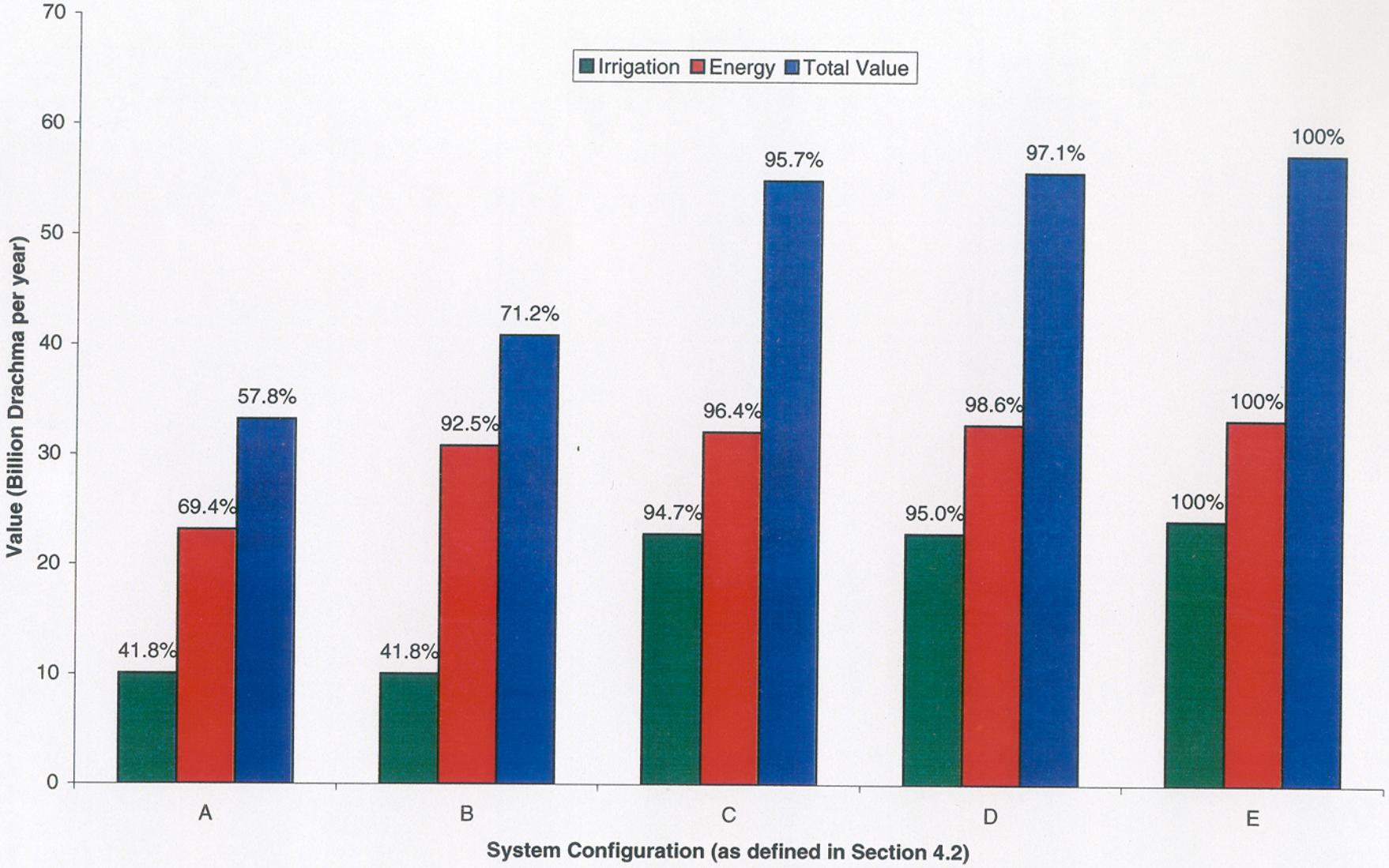

Figure 5.1: Assessment Summary

REFERENCES

Georgakakos, A.P., H. Yao, Y. Yu, and K.G. Noutsopoulos, "A Reservoir Control Model for the Acheloos River," Technical Report No. GIT/CEE-HYDRO-95-6, School of Civil and Environmental Engineering, Georgia Tech, Atlanta, September 1995, 124p.

Georgakakos, A.P., Yao, H., and Y. Yu, "A Control Model for Dependable Hydropower Capacity Optimization," *Water Resources Research*, 33(10), 2349-2365, 1997.

Georgakakos, A.P., H. Yao, and Y. Yu, "Control Models for Hydroelectric Energy Optimization," *Water Resources Research*, 33(10), 2367-2379, 1997.

Georgakakos, A.P., H. Yao, and Y. Yu, "A Control Model for Hydroelectric Energy Value Optimization," *ASCE J. for Wat. Res. Plan. and Mgt,* 123(1), 30-38, 1997.

APPENDIX A

RESERVOIR DATA AND CHARACTERISTICS

A.1 Elevation vs. Storage Relationships

Table A.1.1: Elevation vs. Storage Data for Mesohora

Level (m)	Area (km^2)	Storage (mcm)
640	0	0
650	0.055	0.09
660	0.24	1.56
670	0.515	5.33
680	0.925	12.53
690	1.355	23.93
700	1.873	40.07
710	2.59	62.38
720	3.22	91.43
730	3.985	127.45
740	4.751	171.13
750	5.671	223.26
760	6.738	285.28
770	7.823	358.08
780	8.983	442.11
790	10.166	537.85
800	11.57	646.53

Table A.1.2: Elevation vs. Storage Relationship for Mesohora

Mesohora	
Curve	$H = a + b\,S + c\,\ln S + d\,S^{0.5} + e / S$
Units	H: meters S : million cubic meters
Coefficient	a = +650.5306 b = -0.03702 c = +3.6727 d = +5.8785 e = +0.5903
Validity Range	H: 650-800 meters S : 0.09-646.53 million m^3
Residual Error St. Dev.	0.12 meters

Table A.1.3: Area vs. Storage Relationship for Mesohora

Mesohora	
Curve	$A = a + b\,S + c\,\ln S + d\,S^{0.5} + e / S$
Units	A: square kilometers S : million cubic meters
Coefficient	a = -0.14509 b = +0.005630 c = -0.08873 d = +0.3400 e = -0.01046
Validity Range	A: 0.055-11.57 square kilometers S : 0.09-646.53 million m^3
Residual Error St. Dev.	0.03 square kilometers

Table A.1.4: Elevation vs. Storage Data for Sykia

Level (m)	Area (km^2)	Storage (mcm)
410	0	0
420	0.19	0.6
430	0.417	5.56
440	0.695	8.33
450	1	16.8
460	1.6	22.22
470	2.29	41.66
480	3.17	76.3
490	4.17	111.1
500	5.23	159.4
510	6.46	216.64
520	7.67	287.6
530	9.24	380.52
540	10.98	480.51
550	12.76	590.8

Table A.1.5: Elevation vs. Storage Relationship for Sykia

Sykia	
Curve	$H = a + b\,S + c\,S^{0.5} + d / S$
Units	H: meters S : million cubic meters
Coefficient	a = +434.1881 b = -0.03886 c = +5.6958 d = -0.5047
Validity Range	H: 460-550 meters S : 22.22-590.8 million m^3
Residual Error St. Dev.	0.48 meters

Table A.1.6: Area vs. Storage Relationship for Sykia

Sykia	
Curve	$A = a + b\,S + c\,S^{0.5} + d / S$
Units	A: square kilometers S : million cubic meters
Coefficient	a = -0.1260 b = +0.009174 c = +0.3055 d = +1.7637
Validity Range	A: 1.6-12.76 square kilometers S : 22.22-590.8 million m^3
Residual Error St. Dev.	0.06 square kilometers

Table A.1.7: Elevation vs. Storage Data for Kremasta

Level (m)	Area (km^2)	Storage (mcm)
227	40	999
233	45	1420
240	50	1750
250	58	2300
255	61	2600
260	65	2900
265	68	3300
270	71	3650
275	74	4000
282	79	4500

Table A.1.8: Elevation vs. Storage Relationship for Kremasta

Kremasta	
Curve	$H = a + b\,S + c\,\ln S + d / S + e\,S^2$
Units	H: meters S : million cubic meters
Coefficient	a = -1504.4339 b = -0.08284 c = +237.9412 d = +164627.2045 e = +6.0063E-006
Validity Range	H: 227-275 meters S: 999-4000 million m^3
Residual Error St. Dev.	0.2 meters

Table A.1.9: Area vs. Storage Relationship for Kremasta

Kremasta	
Curve	$A = a + b\,S + c\,\ln S + d / S + e\,S^2$
Units	A: square kilometers S : million cubic meters
Coefficient	a = -2400.3441 b = -0.1217 c = +334.4306 d = +248373.3233 e = +7.8233E-006
Validity Range	A: 45-79 square kilometers S : 1420-4500 million m^3
Residual Error St. Dev.	0.2 square kilometers

Table A.1.10: Elevation vs. Storage Data for Kastraki

Level (m)	Area (km^2)	Storage (mcm)
142	23.3	750
142.5	23.5	755
143	23.8	765
143.2	23.9	770
143.5	24.1	775
144	24.2	785
144.2	24.4	800

Table A.1.11: Elevation vs. Storage Relationship for Kastraki

Kastraki	
Curve	$H = a + b\,S + c\,S^2$
Units	H: meters S : million cubic meters
Coefficient	a = +15.4188 b = +0.28734 c = -1.5776
Validity Range	H: 142-144 meters S: 750-785 million m^3
Residual Error St. Dev.	0.3 meters

Table A.1.12: Area vs. Storage Relationship for Kastraki

Kastraki	
Curve	$A = a + b\,S + c\,S^2 + d / S$
Units	A: square kilometers S : million cubic meters
Coefficient	a = +3050.7503 b = -3.6639 c = +0.001481 d = -834342.3770
Validity Range	A: 23.3-24.4 square kilometers S : 750-800 million m^3
Residual Error St. Dev.	0.03 square kilometers

Table A.1.13: Elevation vs. Storage Data for Stratos

Level (m)	Area (km^2)	Storage (mcm)
64	6.11	43.16
66	6.63	55.79
68	7.05	64.21
70	7.58	84.21

Table A.1.14: Elevation vs. Storage Relationship for Stratos

Stratos	
Curve	$H = a + b\,S + c\,S^2$
Units	H: meters S : million cubic meters
Coefficient	a = +56.5251 b = +0.1974 c = -4.4641E-004
Validity Range	H: 66-75.4 meters S: 55.79-139.5 million m^3
Residual Error St. Dev.	0.1 meters

Table A.1.15: Area vs. Storage Relationship for Stratos

Statos	
Curve	$A = a + b\,S + c\,S^2$
Units	A: square kilometers S : million cubic meters
Coefficient	a = +0.89997 b = +0.1486 c = -8.2270E-004
Validity Range	A: 6.63-7.58 square kilometers S : 55.79-84.21 million m^3
Residual Error St. Dev.	0 square kilometers

Table A.1.16: Elevation vs. Storage Data for Pyli

Level (m)	Area (km^2)	Storage (mcm)
264	0	0
280	0.11	0.64
300	0.78	9.54
320	1.66	33.94
340	2.82	78.74
360	3.4	140.94

Table A.1.17: Elevation vs. Storage Relationship for Pyli

Pyli	
Curve	$H = a + b\,S + c\,S^{0.5} + d / S$
Units	H: meters S : million cubic meters
Coefficient	a = +277.7938 b = -0.04569 c = +7.4586 d = -2.3913
Validity Range	H: 280-360 meters S : 0.64-140.94 million m^3
Residual Error St. Dev.	0.2 meters

Table A.1.18: Area vs. Storage Relationship for Pyli

Pyli	
Curve	$A = a + b\,S + c\,S^{0.5} + d / S$
Units	A: square kilometers S : million cubic meters

Coefficient	a = -0.6967 b = -0.01225 c = +0.4932 d = +0.2697
Validity Range	A: 0.11-3.4 square kilometers S : 0.64-140.94 million m^3
Residual Error St. Dev.	0.07 square kilometers

Table A.1.19: Elevation vs. Storage Data for Mouzaki

Level (m)	Area (km^2)	Storage (mcm)
205	0	0
220	0.51	2.55
240	2.01	26.08
260	3.76	82.81
280	5.38	173.68
300	7.54	302.21
320	9.58	472.94
340	11.89	687.21
360	14.43	949.94

Table A.1.20: Elevation vs. Storage Relationship for Mouzaki

Mouzaki	
Curve	$H = a + b\,S + c\,S^{0.5} + d / S$
Units	H: meters S : million cubic meters
Coefficient	a = +213.9592 b = -0.01552 c = +5.2161 d = -5.7322
Validity Range	H: 220-360 meters S : 2.55-949.94 million m^3
Residual Error St. Dev.	0.04 meters

Table A.1.21: Area vs. Storage Relationship for Mouzaki

Mouzaki	
Curve	$A = a + b\,S + c\,S^{0.5} + d / S$
Units	A: square kilometers S : million cubic meters
Coefficient	a = +0.05750 b = +0.003028 c = +0.3727 d = -0.3850
Validity Range	A: 0.51-14.43 square kilometers S : 2.55-949.94 million m^3
Residual Error St. Dev.	0.06 square kilometers

A.2 Power Functions

Table A.2.1: Power function for Mosohora

Power (MW)	Discharge (m^3/s)	Gross Head (m)
120	81.37	181
123	82.39	184
128	83.5	188
133	84.81	192
138	86.25	196
143	87.48	200
147	88.77	204
152	90	208
156	90	212
159	90	216
163	90	220

Table A.2.2: Power vs. Head Relationship for Mesohora

Mesohora	
Curve	$P = a + b\,H + c\,H^2$
Units	H: meters P : MW
Coefficients	a = -297.7802 b = +3.2760 c = -0.005367
Validity Range	H: 181-220 meters
Residual Error St. Dev.	0.4 MW

Table A.2.3: Discharge vs. Head Relationship for Mesohora

Mesohora	
Curve	$Q = a + b\,H + c\,H^2$
Units	H : meters Q : m^3/s
Coefficients	a = -181.2770 b = +2.4426 c = -0.005491
Validity Range	H: 181-220 meters
Residual Error St. Dev.	0.4 m^3/s

Table A.2.4: Power function for Sykia

Power (MW)	Discharge (m^3/s)	Gross Head (m)
95	127.23	89
101	127.23	94
107	127.23	99
114	127.23	104
120	127.23	109
126	127.23	114
132	127.23	119
137	126.26	124
138	122.16	129
138	117.82	134
138	113.86	139
138	110.24	144
138	106.90	149
138	103.78	154

Table A.2.5: Power vs. Head Relationship for Sykia

Sykia	
Curve	$P = a + b\,H + c\,H^2 + d\,\ln H,\ H < 129$ $P = 138,\ H >= 129$
Units	H: meters P : MW
Coefficients	a = +6401.8919 b = +41.1680 c = -0.09658 d = -2050.8668
Validity Range	H: 89-129 meters
Residual Error St. Dev.	0.5 MW

Table A.2.6: Discharge vs. Head Relationship for Sykia

Sykia	
Curve	$Q = a + b\,H + c\,H^2 + d / H,\ H > 119$ $Q = 127.23,\ H <= 119$
Units	H : meters Q : m^3/s
Coefficients	a = +4604.8269 b = -32.8957 c = +0.07828 d = -198881.5428
Validity Range	H: 119-154 meters
Residual Error St. Dev.	0.4 m^3/s

Table A.2.7: Specific Generation Efficiency vs. Elevation Data for Kremasta

H (m)	227	229	233	237	241	245	249	253	261	265	271	277	283
E (m^3/kwh)	5.5	5.3	5	4.7	4.4	4.2	4	3.8	3.6	3.2	3	2.8	2.6

Table A.2.8: Specific Generation Efficiency vs. Elevation Relationship for Kremasta

Kremasta	
Curve	$F = a + b\,H + c\,H^2$
Units	H: meters F : cubic meters/KWH
Coefficients	a = +44.082296 b = -0.2666675 c = $+4.2471138 \times 10^{-4}$
Validity Range	H: 227-282 meters
Residual Error St. Dev.	0.01 cubic meters/KWH

Table A.2.9: Specific Generation Efficiency vs. Elevation Data for Kastraki

H (meters)	142	142.5	143	143.5	144	144.5	145.0
E (cubic m^3/kwh)	5.95	5.87	5.78	5.71	5.62	5.56	5.48

Table A.2.10: Specific Discharge vs. Elevation Relationship for Kastraki

Kastraki	
Curve	$F = a + b\,H + c\,H^2$
Units	H: meters F : cubic meters/KWH
Coefficients	a = +136.0164310 b = -1.65976 c = +5.2380953 $x10^{-3}$
Validity Range	H: 142-144.2 meters
Residual Error St. Dev.	0.01 cubic meters/KWH

Table A.2.11: Specific Generation Efficiency vs. Elevation Data for Stratos

H (m)	67	67.5	68	68.5	69
E (m^3/kwh)	11.7	11.54	11.39	11.24	11.10

Table A.2.12: Specific Discharge vs. Elevation Relationship for Stratos

Stratos	
Curve	$F = a + b\,H + c\,H^2$
Units	H: meters F: cubic meters/KWH
Coefficients	a = +84.632 b = -1.8542 c = $+1.14285 \times 10^{-2}$
Validity Range	H: 142-144.2 meters
Residual Error St. Dev.	0.01 cubic meters/KWH

Table A.2.13: Power function for Mouzaki

Generation			Pumping		
Power (MW)	Discharge (m^3/s)	Gross Head (m)	Power (MW)	Discharge (m^3/s)	Gross Head (m)
170	236.12	94	313	273.52	94
184	238.70	98	314	266.87	98
195	241.04	102	314	260.19	102
207	243.58	106	314	253.50	106
219	245.61	110	314	246.78	110
231	247.74	114	313	240.03	114
243	249.93	118	313	233.27	118
253	251.37	122	312	226.48	122
265	254.27	126	312	219.66	126
276	256.20	130	311	212.82	130
286	258.12	134	309	205.96	134

Table A.2.14: Power vs. Head Relationship for Mouzaki

Mouzaki	
Curve	$P = a + b\,H + c\,H^2$
Units	H: meters P : MW
Coefficients	a = -182.4548 b = +4.3570 c = -0.006410
Validity Range	H: 94-134 meters
Residual Error St. Dev.	0.5 MW

Table A.2.15: Discharge vs. Head Relationship for Mouzaki

Mouzaki	
Curve	$Q = a + b\,H + c\,H^2$
Units	H : meters Q : m^3/s
Coefficients	a = +167.4229 b = +0.8646 c = -0.001404
Validity Range	H: 94-134 meters
Residual Error St. Dev.	0.2 m^3/s

Table A.2.16: Power function for Pefkofito

Generation			Pumping		
Power (MW)	Discharge (m^3/s)	Gross Head (m)	Power (MW)	Discharge (m^3/s)	Gross Head (m)
151	104.72	195	195	86.97	195
158	105.80	200	194	84.61	200
171	107.85	210	190	79.84	210
183	109.70	220	185	75.03	220
196	111.37	230	180	70.16	230
208	112.80	240	297	105.68	240
221	114.00	250	295	101.95	250
232	114.00	260	292	98.16	260
244	114.00	270	289	94.18	270
255	114.00	280	284	90.10	280
266	114.00	290	279	85.88	290
277	114.00	300	273	81.55	300

Table A.2.17: Power vs. Head Relationship for Pefkofito

Pefkofito	
Curve	$P = a + b\,H + c\,H^2$
Units	H: meters P : MW
Coefficients	a = -153.3011 b = +1.7969 c = -0.001209
Validity Range	H: 195-300 meters
Residual Error St. Dev.	0.3 MW

Table A.2.18: Discharge vs. Head Relationship for Pefkofito

Pefkofito	
Curve	$Q = a + b\,H + c\,H^2$, $H < 250$ $Q = 114$, $H >= 250$
Units	H : meters Q : m^3/s
Coefficients	a = +21.3012 b = +0.6293 c = -0.001034
Validity Range	H: 195-250 meters
Residual Error St. Dev.	0.01 m^3/s

APPENDIX B

THE PUMP-DISCHARGE OPERATION OF PEFKOFITO

B.1. Introduction

One of the objectives of this study is to evaluate the benefit of installing a reversible-shaft turbine at the Pefkofito power facility between the reservoirs of Sykia and Mouzaki. This would allow a pump-storage operation between these two reservoirs by discharging water from Sykia to Mouzaki during the peak hours and recharging the former reservoir during off-peak hours. For each period considered, the feasibility of this operation is constrained by several elements, the most important of which are as follows:

1. Net transfer between the reservoirs of Sykia and Mouzaki during the period (U);
2. Net head between the two reservoirs (H);
3. Maximum number of hours of primary energy generation in the period (MTPK);
4. Maximum number of hours of recharging operations in the period (MTPM);
5. Unit price of primary energy (Λp);
6. Unit cost of the energy required for pumping operations (Λs);

The value of U determines what fraction of the peak time is required for transfer the water directed to Thessalia and what fraction, if any, can be used for discharging the water pumped back from Mouzaki. H constrains the efficiency of Pefkofito operations both in generating and in recharging mode and the hourly amount of water that can be passed through the station in either direction. The ratio between Λp and Λs is a fundamental factor affecting the convenience of the pumping/discharge operation.

One strategic assumption that was done in this study is that the unit cost of the energy required for pumping operations (Λs) is equal to the unit price of the energy produced during off-peak hours (named secondary energy). The rational behind this assumption is that recharging is performed during off-peak hours either by buying energy from external sources at market price or by using energy produced within the Acheloos system. In both cases, there is a loss of income to the system operator either due to actual payment of external suppliers or to the missed revenue from the sale of the secondary energy used for pumping.

Another fundamental assumption that was made is that H remains constant during the time step. Thus, there is no convenience to use the pumping operations for keeping high the net head between the two reservoirs.

Any feasible set of the parameters U, H, MTPK, MTPM, Λp, and Λs can produce three alternative outcomes:

1. The value of U is so large that all the primary generation and maybe some part of the secondary time is required for diverting water to Thessalia;
2. The value of U is small enough that additional water could be discharged during peak hours, but the ratio Λp/Λs and the turbine efficiencies make the pump-storage operation not economically convenient;
3. The value of U is small enough that additional water could be discharged during peak hours and the ratio Λp/Λs and the turbine efficiencies make the pump-storage operation economically profitable.

The number of hours required to pass the net discharge U trough Pefkofito power station is given by:

$$\frac{U \cdot 10^{6}}{Q(H) \cdot 3600},$$

where U = Net transfer between the reservoirs of Sykia and Mouzaki and later to Thessalia (MCM)

Q(H) = Maximum discharge through Pefkofito in generation mode for a given net head H (m^3/s)

If this number is higher than MTPK, then there is no room for allocating additional primary generation (case 1). Consequently, the additional value of the pump-storage operation would be nil. If this number is lower than MTPK, the economical profitability of the pump-storage operation is assessed through the following function:

$$POW(H) - POW_{PUMP}(H) \cdot \frac{Q(H)}{Q_{PUMP}(H)} \cdot \frac{\Lambda s}{\Lambda p}$$

where POW(H) = Power generated by the Pefkofito power station in generation mode for a given net head H (MW);

$POW_{PUMP}(H)$ = Power required by the Pefkofito power station in recharging mode for a given net head H (MW);

$Q_{PUMP}(H)$ = Maximum discharge through Pefkofito in generation mode for a given net head H (m^3/s)

If the outcome of this function is negative, then the pump-storage operation is not profitable (case 2) and the additional value of the pump-storage operation is nil. Once that the physical and economical feasibility of the pump-storage operation has been ensured, the additional primary production of energy by pump-storage operation is limited either by the time available for additional

primary generation or by the time available for recharging operations. The first possibility is given when:

$$Q_{PUMP}(H) \cdot MTPM \cdot 3600 + U \cdot 10^6 > Q(H) \cdot MTPK \cdot 3600$$

In this case the additional hours of primary energy generation is given by:

$$NADDHR = MTPK - \frac{U \cdot 10^6}{Q(H) \cdot 3600}$$

Alternatively, the recharging operation is the limiting factor and the additional primary generation time is given by:

$$NADDHR = \frac{Q_{PUMP}(H) \cdot MTPM \cdot 3600}{Q(H) \cdot 3600}$$

In either case, the additional value produced by the pump-storage operation is given by:

$$\Lambda p \cdot \left(POW(H) - POW_{PUMP}(H) \cdot \frac{Q(H)}{Q_{PUMP}(H)} \cdot \frac{PRPM}{PRPK} \right) \cdot NADDHR$$

This value is the difference between the value of the additional primary energy produced and the cost of the recharging operation. If this value is divided by the primary energy price, the result has the dimension of energy and represents the gain in valuable energy obtained by operating the pump-storage scheme during the period. This value is defined as Modified Energy and is represented in Figures B1, B2, and B3 for three different ratios between Λp and Λs. The time step is one month, the weekly primary generation time is six hours per day in seven days per week and the maximum time that can be devoted to recharge operations is eight hours per day.

The discontinuity in the Modified Energy corresponding to the Net Head of 230 m is due to the discontinuity in the characteristics of the Pefkofito pumping station (Table B.2.7) and is not very relevant for price ratios of 12/4 and 12/6, while its effect is more notable for the ratio 12/8.

Note that although the magnitude of the net transfers between Sykia and the Thessalia can reach 600 MCM, above 80 MCM per month, there is no room for additional pump-storage operations setting the additional Modified Energy to zero.

B.2. Analytical Approximation of the Modified Energy Function

The Modified Energy function defined above multiplied by the primary energy price gives the additional value produced by the pump-storage operation. Consequently, this item must be added to the primary and secondary energy production terms of the performance index of the whole system. Figures B1, B2, and B3 show that this type of function is not compatible with the ELQG algorithm since it is neither concave nor convex. Further, the ELQG requires the computation of the partial derivatives of this function with respect to both U and H. Consequently, for taking into account the pumping operation in the optimization scheme, it is necessary to provide an analytical approximation of the Modified Energy as a function of H and Q. After several trials, it was found that the function that best approximate the Modified Energy is the following:

$$ME = \begin{cases} a + b \cdot H + c \cdot U + d \cdot H^2 + e \cdot U^2 + f \cdot HU + g \cdot H^3 + h \cdot H^2U + i \cdot U^3 \; j \cdot HU^2 \\ \qquad\qquad\qquad\qquad\qquad\qquad\qquad\qquad\qquad\qquad\qquad\qquad\qquad\qquad for \;\; U_l \le U \le U_h, H_l \le H \le H_h \\ 0 \quad otherwise \end{cases}$$

The regression coefficients, the coefficient of determination and the standard error for the three price ratios illustrated in Figures B4, B5, and B6 are reported in Table B1.

Table B1: Parameters of the formulas approximating the Modified Energy for three ratios Δp/Δs.

Parameter	Ratio 12/4	Ratio 12/6	Ratio 12/8
a	27149.57538	41509.46107	239418.7386
b	-332.3400077	-469.7363209	-2798.027498
c	29.47341033	-154.9023392	244.676185
d	1.776600516	1.88532383	10.63960392
e	-2.05313611	-1.21210464	-0.46749292
f	-0.388573068	1.493114401	-0.90770931
g	-0.002237409	-0.002022668	-0.013092031
h	-0.002406595	-0.005259886	-0.000279906
i	0.022284845	0.011845977	0.001790404
j	-0.000697758	0.000088508	0.001059392
U_l	0.0	0.0	0.0
U_h	80.0	80.0	80.0
H_l	195.0	195.0	245.0
H_h	300.0	300.0	300.0
r^2	0.998879181	0.997828126	0.99526467
Standard error	263.6569103	201.8873745	75.21999286

Regression has been performed ignoring the values of the Modified Energy around the discontinuity (Net head = 230 and 235) and giving more weight to the values corresponding to a head above 235 m. For the 12/8 price ratio, regression has been performed considering only values of head above 240 m. The values of the coefficient of determination and the standard error reported in Table A1 refer to this portion only and do not take into consideration the small bump between H = 210 and H = 230 m. The coefficients of determination and the value of the standard errors reported in Table B1 and the charts represented in Figures B1, B2, and B3 show that the regression functions track the original functions very closely, especially for values of the H above 235 m. The major errors are for the 12/4 and 12/6 ratios those corresponding to Net head between 230 and 235 m; for the 12/8 ratio, the major errors are caused by H between 210 and 230 m.